UCSF
UC San Francisco Electronic Theses and Dissertations

Title
Autophagy-Independent Senescence and Genome Instability Driven by Targeted Telomere Dysfunction

Permalink
https://escholarship.org/uc/item/52h777ts

Author
Mar, Florie

Publication Date
2015

Peer reviewed|Thesis/dissertation

eScholarship.org Powered by the California Digital Library
University of California

Autophagy-Independent Senescence and Genome Instability Driven by Targeted Telomere Dysfunction

by

Florie Anne Mar

DISSERTATION

Submitted in partial satisfaction of the requirements for the degree of

DOCTOR OF PHILOSOPHY

in

Biomedical Sciences

in the

GRADUATE DIVISION

of the

UNIVERSITY OF CALIFORNIA, SAN FRANCISCO

[redacted]

Copyright 2015

by

Florie Anne Mar

Dedication

I dedicate this work to Jordan Mar, my wonderful husband and biggest supporter who was by my side through it all

And to the memory of my loving mother, Anne-Henriette Charles, who has been my inspiration and a powerful source of motivation

ACKNOWLEDGEMENTS

First, I would like to thank my graduate advisor, Bradley Stohr, for his wonderful scientific guidance and support throughout this project. I am thankful for his mentorship, his availability, and his scientific rigor, which have taught me how to design, conduct, and interpret the most pertinent questions to derive knowledge that others can build on. Even when things were tough, Brad was able to draw the good from any situation and help me design a plan to move forward. None of this would have been possible without Brad's mentorship and guidance.

I would also like to thank my co-mentor, Jay Debnath, who has provided much needed scientific input into the field of autophagy. I truly appreciate Jay's ability to take a step back and build a story from data that may feel disjointed.

I would also like to thank the rest of my thesis committee, Elizabeth Blackburn and Andrei Goga, for providing unique scientific insight, guidance, and inspiration. Their outside perspective was instrumental for the success of this project as they helped turn this study into a meaningful piece of biology that moves our field forward.

I would like to thank my lab: Ajay and Morgan. Ajay and Morgan have helped me conduct and interpret experiments, move forward when experiments were bringing me down, and find a way to make it all make sense. Their friendships have made my time in the lab so much more enjoyable.

Next, I'd like to thank the members of the Debnath lab, both past and present. The Debnath lab taught me a tremendous amount about the field of autophagy, shared their expertise with me, and provided essential feedback for my project. Special thanks to Candia, Lyndsay, and Jenny for helping me in tough times and for always being there

to listen to my autophagy troubles. I am so thankful to have had the opportunity to collaborate with Jenny over the past few years and contribute to her project. I have learned so much from her about science, both technically and conceptually.

I'd also like to thank all of the friends that have helped me through these past five years. Some are in San Francisco, others live elsewhere around the world, but all have been there to listen to me and support me through the ups and downs. Thank you Loriane Holliday, Victoria Sauveplane, Manon Guillermin, Anna Gillespie, Sam Bell, Miranda Broz, Marie Grob, Bevin English, Craig Dewitt, and many more.

Thank you to my family for their love and support throughout these years. I'm so happy to have my wonderful siblings Alix, Geoffrey, and Emeric in San Francisco and I'm thankful for their love and friendship, which have been crucial to my success at UCSF. A big thank you to Papa who motivated and inspired me to higher heights. He has been an incredible source of support and I'm thankful for his continued belief in me. Thank you to the Mar's for taking me into their family and being there for me from the very start. I'm thankful for the love and support I've received from Julie and Terry over the years, from dinner parties, to afternoon visits, to cabin weekends. Natalie, Andrew, Jen, and Nathan, thank you for being great friends and helping me get to this point.

And finally, I would like to thank Jordan for believing in me, for putting up with me, and for being by my side throughout this entire journey. It's truly been a roller coaster and I'm so thankful to have had him there to pick me up and to push me to think bigger and further. He has been my biggest champion, source of support, and a major part of my successes. None of this would have been possible without him and I will strive to ensure that his confidence and belief in my abilities are well deserved.

Contributions to presented work

The work described in this dissertation was done under the direct supervision and guidance of Dr. Bradley Stohr.

Contents in Chapters 1-4 are modified from the following publication:
Mar, FA, Debnath, J., Stohr BA. (2015). Autophagy-independent senescence and genome instability driven by targeted telomere dysfunction. *Autophagy, 11*(3): 527-37

The co-authors listed in this publication directed and supervised the research that forms the basis for the dissertation.

Jayanta Debnath performed the experiments that led to the creation of Figure S1. Florie Mar performed all other experiments described in this dissertation.

Autophagy-Independent Senescence and Genome Instability Driven by Targeted Telomere Dysfunction

Florie Anne Mar

ABSTRACT

Telomere dysfunction plays a complex role in tumorigenesis. While dysfunctional telomeres can block the proliferation of incipient cancer clones by inducing replicative senescence, fusion of dysfunctional telomeres can drive genome instability and oncogenic genomic rearrangements. Therefore, it is important to define the regulatory pathways that guide these opposing effects. Autophagy is a highly conserved stress response pathway that degrades cytoplasmic components and, in recent work, has been shown to regulate both senescence and genome instability in various contexts.

In this study, we apply models of acute telomere dysfunction to determine whether autophagy modulates the resulting genome instability and senescence responses. While telomere dysfunction rapidly induces autophagic flux in human fibroblast cell lines, inhibition of the autophagy pathway does not have a significant impact on the transition to senescence, in contrast to what has previously been reported for oncogene-induced senescence. Our results suggest that this difference may be explained by disparities in the development of the senescence-associated secretory phenotype as a result of different levels of DNA damage. We also show that chromosome fusions induced by telomere dysfunction are comparable in autophagy-proficient and autophagy-deficient cells. Altogether, our results highlight the complexity

of the senescence-autophagy interface and indicate that autophagy induction is unlikely to play a significant role in telomere dysfunction-driven senescence and chromosome fusions.

Chapter 1 provides an overview of the autophagy and senescence pathways as well as the research available to date linking autophagy to senescence and genome instability with a focus on the major open questions. In Chapter 2, I will present data identifying the autophagy-independent nature of senescence triggered by targeted telomere dysfunction. In Chapter 3, I will present data defining the autophagy-independent nature of genome instability that results from telomere dysfunction. Finally, Chapter 4 is a discussion of the implications of this work for the fields of telomere dysfunction, senescence, and autophagy in a basic biology and clinical context.

TABLE OF CONTENTS

Chapter 1	Introduction	1
Chapter 2	Telomere dysfunction-induced senescence is autophagy-independent	9
Chapter 3	Genome instability driven by targeted telomere dysfunction is autophagy-independent	49
Chapter 4	Implications and future directions	59
References		66

LIST OF FIGURES

Chapter 2

Figure 1.	Punctate GFP-LC3B in replicative senescent human fibroblasts	12
Figure S1.	Punctate GFP-LC3B during HMEC agonescence	13
Figure 2.	Autophagy is induced in response to telomere dysfunction from MT-hTER-47A	16
Figure S2.	Autophagic flux is induced in response to MT-hTER compared to vector or WT-hTER	18
Figure 3.	Autophagy inhibition does not affect the senescence transition following MT-hTER-47A treatment of WI-38 fibroblasts	20
Figure S3.	Autophagy inhibition does not affect MT-hTER-induced senescence in WI-38 fibroblasts	22
Figure 4.	Autophagy inhibition does not affect the senescence transition following MT-hTER-47A treatment of BJ fibroblasts	25
Figure S4.	shRNA-mediated *ATG* silencing in BJ fibroblasts	27
Figure 5.	Senescence transition in the absence of a robust SASP in MT-hTER-47A-expressing BJ fibroblasts	30
Figure S5.	Senescence transition in the absence of a robust SASP is a common feature of several forms of TDIS in BJ-TERT fibroblasts	32
Figure 6.	Cells expressing the v-cyclin oncogene have higher levels of DNA damage than those with telomere dysfunction	36
Figure 7.	Levels of DNA damage positively correlate with levels of secreted IL6 and IL8 during early senescence	40

Chapter 3

Figure 1.	Autophagy inhibition does not affect genomic instability following MT-mTER-47A or Tpp1$^{\Delta RD}$ transduction	54

CHAPTER 1

Introduction

Content in this chapter was modified from the following publication:

Mar, FA, Debnath, J., Stohr BA. (2015). Autophagy-independent senescence and genome instability driven by targeted telomere dysfunction. *Autophagy, 11*(3): 527-37

TELOMERE DYSFUNCTION AND TUMORIGENESIS

Telomeres are composed of specialized DNA and associated proteins. They consist of tandem TTAGGG DNA repeats that maintain genome stability by recruiting protein complexes called shelterins, which protect chromosome ends from recognition as double-strand DNA breaks. Telomeres are maintained by the enzyme telomerase, composed of a protein component TERT (telomerase reverse transcriptase) and an RNA component TER (telomerase RNA component). TERT uses the TER RNA template to catalyze the addition of new telomeric repeats at the telomere end.

Upon extensive loss of telomeric sequence, which can occur progressively because of replicative shortening (L. Hayflick, 1961), the resulting dysfunctional telomeres activate a canonical DNA damage response (Fabrizio d'Adda di Fagagna, 2003) that promotes senescence and/or genome instability depending upon the cellular context. Telomere dysfunction-induced senescence (TDIS) is an important barrier to tumor development because it can block the proliferation of incipient cancer cells (Anitha Suram, 2012; Jerry W. Shay, 2005). However, telomere dysfunction can also induce genome-destabilizing chromosome fusions that promote tumor initiation, progression, and evolution (Ding Z, 2012; Eros Lazzerini Denchi, 2007; Susan M. Bailey, 2006).

In order to maintain replicative potential, cancer cells maintain telomere integrity by overexpressing TERT—found in 90% of human cancers—or through alternative lengthening of telomeres—a mechanism that uses homologous recombination to extend the telomeric sequence. Interestingly, recent human genetic studies suggest that

alteration of telomeric maintenance control is an important early event in tumor development (Franklin W. Huang, 2013; João Vinagre, 2013; Patrick J. Killelaa, 2013; Robert J. A. Bell, 2015; Sumit Borah, 2015; Susanne Horn, 2013). These studies discovered mutations in the TERT promoter that generate novel transcription factor binding sites (Robert J. A. Bell, 2015) that increase TERT expression and telomerase activity, and identified TERT promoter mutations as the most common genetic mutations in many cancers, including 83% of glioblastomas (Robert J. A. Bell, 2015) and 74% of metastatic melanomas (Susanne Horn, 2013). The high prevalence of these TERT promoter mutations and their widespread occurrence as somatic mutations in several kinds of human cancers suggests that telomere crisis is an early event in tumor development. By increasing cellular replicative potential, these TERT promoter mutations may increase the pool of cells available for further cancer progression events. Thus, mutations that reactivate telomerase appear to be drivers for early cancer initiation.

Telomere dysfunction plays a multi-faceted role in tumorigenesis, both promoting and blocking early cancer development depending on the cellular context. One of the goals of this study is to better understand the pathways required for defining the pro- or anti-tumorigenic properties of telomere dysfunction.

MECHANISMS OF CELLULAR SENESCENCE

Replicative senescence refers to the essentially irreversible cell cycle arrest triggered by telomere erosion from replicative exhaustion (L. Hayflick, 1961). Senescence is mediated by two major molecular signaling pathways—p53/p21 and $p16^{INK4a}$/pRB. Although senescence is considered irreversible, molecular manipulations of these signaling pathways can reverse the senescent state. Interestingly, researchers found that, in cells expressing low p16 at senescence, loss of p53 reverses replicative senescence. On the other hand, cells that senesce in the presence of high p16 cannot resume growth upon loss of p53 (Christian M. Beauséjour, 2003). Growth arrest induced by senescence is an important barrier to tumorigenesis that limits the growth of potential precancerous cells.

The senescent state is also associated with widespread changes in chromatin organization and gene expression, leading to the development of the senescence associated secretory phenotype (SASP). The SASP is a collection of secreted pro-inflammatory cytokines, growth factors, and proteases that both reinforce the senescence growth arrest (Thomas Kuilman, 2008) and promote epithelial-mesenchyme transition and invasiveness through paracrine signaling (Jean-Philippe Coppé, 2008) .

In addition to telomere dysfunction, cellular senescence can be triggered by constitutive activation of oncogenes such as $HRAS^{G12V}$ (Manuel Serrano, 1997), or loss of tumor suppressors including PTEN (Zhenbang Chen, 2005). Similar to TDIS, oncogene-induced senescence (OIS) is proposed to be an important barrier to tumor

progression and to be caused, at least in part, by a DNA damage response secondary to replication stress (Chrysiis Michaloglou, 2005; Jerry W. Shay, 2005; Jirina Bartkova, 2006; Melanie Braig, 2005; Raffaella Di Micco, 2006). Nonetheless, there are fundamental differences between these two types of senescence (Jirina Bartkova, 2006; Raffaella Di Micco, 2006). First, OIS can occur independently of a DNA damage response (Haferkamp S, 2009). Second, OIS and TDIS exhibit qualitatively and quantitatively distinct gene expression profiles, with differences in expression of Wnt target genes and chromatin regulators (Nelson DM, 2014). Finally, while both OIS and TDIS induce secretion of myriad cytokines and other factors as part of the senescence-associated secretory phenotype (SASP), the SASP differs both in magnitude and composition between these two modes of senescence (Jean-Philippe Coppé, 2008; Thomas Kuilman, 2008).

AUTOPHAGY AS A SENESCENCE MEDIATOR

Macroautophagy (hereafter referred to as autophagy) is a catabolic process that plays a central role in ensuring proper cellular homeostasis as well as survival in response to stress (Debnath, 2013). During activation of autophagy, a double membrane structure called the autophagosome sequesters long-lived proteins, damaged organelles, or other cargo to be degraded upon fusion of the outer membrane of the autophagosome with the lysosome. By clearing damaged organelles, autophagy prevents oxidative stress and inflammation.

Autophagy is tightly controlled by several highly conserved genes called *ATGs* (AuTophaGy genes). Two ubiquitin-like conjugation systems play key roles in regulating early autophagosome formation. First, the ubiquitin-like ATG12 is activated by the E1-like ATG7 enzyme and transferred to the E2-like conjugating enzyme ATG10 for subsequent attachment to ATG5. Next, ATG7 and ATG3 conjugate LC3 to a phosphatidylethanolamine, forming LC3-II. LC3-II subsequently associates with the membrane of the developing autophagosome and is used as a marker of autophagy (Debnath, 2013). Loss of any of these ATG proteins results in the complete ablation of the autophagy pathway (Noboru Mizushima, 2010).

In addition to maintaining cellular homeostasis, autophagy is also activated in response to a variety of cellular stresses, including growth factor withdrawal, hypoxia, pathogenic infection, and DNA damage (Guido Kroemer, 2010). As a stress response pathway, autophagy recycles cargo to insure the availability of nutrients and energy needed to overcome the stressor, such as providing amino acids for *de novo* protein synthesis.

Recently, autophagy has been uncovered as an important regulator of OIS because of its role in supporting the production of a robust SASP that promotes the senescence transition in response to oncogenic $HRAS^{G12V}$ or Kaposi sarcoma-associated herpesvirus cyclin (v-cyclin) (Andrew M. Leidal, 2012; Andrew R.J. Young, 2009; Masako Narita, 2011; Thomas Kuilman, 2008). However, other studies suggest that autophagy can block senescence in certain circumstances, highlighting the complex relationship between autophagy and senescence (Gewirtz, 2013; Hyun Tae Kang, 2011; Yihua Wanga, 2012). Although increased autophagy has been observed in

response to dysfunctional telomeres, the role of autophagy in TDIS remains unclear (Hiroshi Aoki, 2007; Nicola Ivan Orlotti, 2012; Wen-Jun Zhou, 2009). One of the goals of this work is to define the role of autophagy in TDIS induced by a targeted form of telomere dysfunction.

AUTOPHAGY AND GENOME STABILITY

Autophagy has also been implicated in the maintenance of genome stability. Initial studies showed that autophagy promotes genome stability by maintaining cellular metabolic homeostasis (Robin Mathew, 2007). More recent work in yeast and mammalian cells suggests that autophagy can directly influence DNA damage repair by modulating levels of the key repair protein CtIP (Praveen Rajendran, 2013; Robert T, 2011). Moreover, autophagy guards against aneuploidy by regulating cell cycle progression and cytokinesis (Aiko Matsui, 2013; Amine Belaid, 2013).

Genome instability triggered by telomere dysfunction results from an attempt to repair unprotected chromosome ends. The results are end-to-end chromosome fusions that propel cells into breakage-fusion-bridge cycles, resulting in aneuploidy, dicentric chromosomes, or acentric chromosome fragments that contribute to genome instability (Lange, 2005). Genome instability triggered by telomere dysfunction can be a source for new oncogenic mutations that drive cells one step closer to malignant transformation (Susan M. Bailey, 2006). Because autophagy plays a role in DNA damage repair—an important pathway that produces genome instability downstream of telomere

dysfunction—autophagy may play a role in the extent or types of genome instability that result from targeted telomere dysfunction.

In light of these emerging roles for autophagy in senescence and genome instability, two critical sequelae of telomere dysfunction, we sought to delineate the potential functions of autophagy in the cellular response to acute telomere dysfunction.

In Chapter 2, I present work demonstrating the autophagy-independent nature of senescence driven by targeted telomere dysfunction. In addition, I will describe our work identifying several key differences in the levels of DNA damage signaling and SASP development that depend on the senescence trigger. In Chapter 3, I present data revealing the autophagy-independent nature of genome instability in response to targeted telomere dysfunction. Overall, these results highlight the complex relationship between autophagy and senescence, and demonstrate that the pathways involved in the establishment of senescence depend on the senescence trigger.

CHAPTER 2

Telomere dysfunction-induced senescence is autophagy-independent

Content in this chapter was modified from the following publication:

Mar, FA, Debnath, J., Stohr BA. (2015). Autophagy-independent senescence and genome instability driven by targeted telomere dysfunction. *Autophagy, 11*(3): 527-37

SUMMARY

Autophagy mediates the transition to senescence induced by several oncogenes, including Ras and v-cyclin. We sought to interrogate the role of the autophagy pathway in mediating the senescence response induced by telomere dysfunction. The data presented here shows that, while targeted telomere dysfunction activates autophagic flux, autophagy is not required for the development of TDIS. Furthermore, we identify several differences between OIS and TDIS that may underlie the different requirement for autophagy in mediating the transition to senescence. First, whereas transition to OIS occurs in the presence of a robust SASP, transition to TDIS occurs in the absence of secreted IL6 and IL8, key SASP factors. Next, OIS features high levels of non-telomeric DNA damage, whereas TDIS is characterized by lower levels of telomeric DNA damage. Lastly, we describe an interesting correlation between levels of IL6 and phosphorylated-ATM, but not phosphorylated-p53, in the early stages of senescence. Overall, these results define the autophagy-independent nature of TDIS and highlight the fact that the pathways and cellular responses responsible for the development of senescence depend on the senescence trigger.

HIGHLIGHTS

- Autophagy is induced in response to a targeted form of telomere dysfunction.
- Loss of autophagy has no impact on telomere dysfunction-induced senescence.
- TDIS is associated with a lower SASP than OIS during senescence transition.
- The levels of DNA damage are positively correlated with the magnitude of the SASP during senescence transition.

RESULTS

Telomere dysfunction induces autophagic flux in human fibroblasts.

To determine whether autophagy is involved in the cellular response to telomere dysfunction, we first examined autophagy status in the context of replicative senescence in WI-38 human fibroblasts. Because WI-38 cells lack telomerase activity, their telomeres shorten during each S phase until reaching a critically short length that induces a DNA damage response and replicative senescence (Fabrizio d'Adda di Fagagna, 2003; L. Hayflick, 1961). As a control, we generated WI-38 cells stably expressing TERT (telomerase reverse transcriptase; WI-38-TERT cells), which confers robust telomerase activity and blocks replicative telomere shortening (Andrea G. Bodnar, 1998). As expected, the primary WI-38 fibroblasts lacking TERT entered replicative senescence over a period of extended culture, while the WI-38-TERT cells proliferated indefinitely (**Figure 1A**). To monitor autophagosome formation during senescence, we used cells that stably express GFP fused to MAP1LC3B/LC3B (microtubule associated protein 1 light chain 3; GFP-MAP1B/LC3B) and observed that the senescent WI-38 fibroblasts showed an increase in GFP-tagged LC3B puncta while the WI-38-TERT cells did not (**Figure 1B**). Similar results were observed in human mammary epithelial cells (HMECs) upon transition to agonescence, a senescence associated growth plateau resulting from telomere dysfunction-induced growth arrest (**Figure S1**) (Paul Yaswen, 2002).

Figure 1

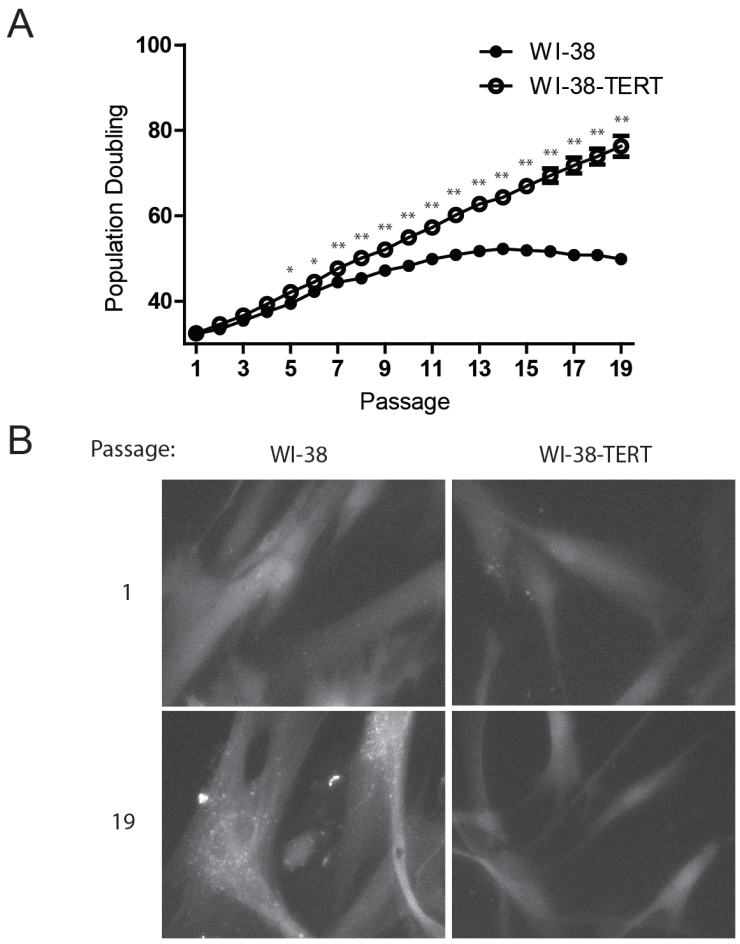

Figure 1. Punctate GFP-LC3B in replicative senescent human fibroblasts.

(**A**) Growth curves of primary WI-38 and WI-38-TERT fibroblasts in extended culture. Error bars represent standard deviation among three wells grown in parallel. (**B**) Representative images of GFP-LC3B puncta in WI-38 or WI-38-TERT cells at passage 1 and 19 after initiation of culture. A 40X objective was used for imaging. * and ** indicate significance at $P<0.05$ and $P<0.01$ respectively.

Figure S1

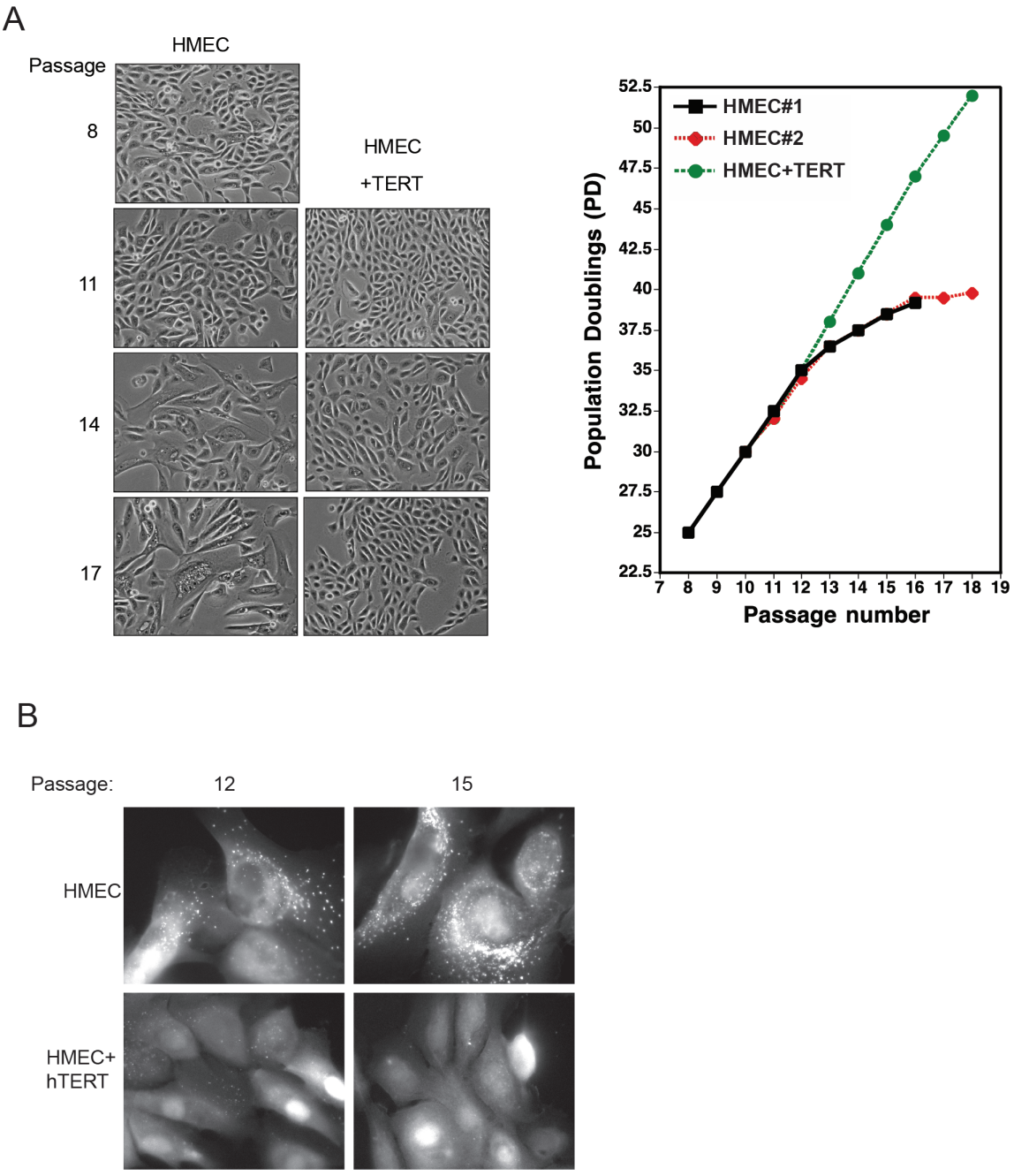

Figure S1. Punctate GFP-LC3B during HMEC agonescence.

(**A**) Representative images and growth curve of HMEC or HMEC-TERT cultures at the indicated passages during extended culture. (**B**) GFP-LC3B puncta in HMEC and HMEC-TERT cells at the indicated passages.

In contrast to OIS, replicative senescence appears gradually as the onset of telomere dysfunction occurs asynchronously within a proliferating cell population (Carmen Martin-Ruiz, 2004; Ian R. Kill, 1994), thereby complicating the rigorous quantification of autophagic flux as well as mechanistic studies of autophagy in this context. Accordingly, to more effectively scrutinize the relationship between telomeric dysfunction and autophagy, we employed a well-defined acute model of TDIS. Telomerase is minimally composed of a TERT protein and a template-containing RNA (TER). We utilized a mutant form of human TER containing base changes in the template region, hereafter referred to as MT-hTER-47A for mutant template *Homo sapiens* TER (or in the case of mice, MT-mTER-47A for mutant template *Mus musculus* TER) (Lidija Marusic, 1997; Moses M. Kim, 2001). When MT-hTER-47A is overexpressed, it joins with endogenous TERT to form mutant telomerase enzyme that adds variant TTTGGG telomeric repeats to chromosome ends (**Figure 2A**), thereby disrupting shelterin binding and inducing acute telomere dysfunction (Lidija Marusic, 1997; Moses M. Kim, 2001). MT-hTER-47A overexpression in WI-38-TERT cells caused rapid telomere dysfunction as demonstrated by the induction of DNA damage foci at telomeres (telomere dysfunction-induced foci, TIFs; **Figure 2B**). Furthermore, MT-hTER-47A induced senescence rapidly and relatively uniformly over a period of 7 to 10 days, as demonstrated by dramatically reduced cell proliferation and the appearance of enlarged cells positive for senescence-associated beta-galactosidase (SA-β-gal; **Figure 2C to E**).

We next asked whether autophagy is induced during MT-hTER-47A-driven senescence. Indeed, an accumulation of GFP-LC3B puncta was observed in MT-hTER-47A expressing cells, but not in vector controls (**Figure 2F**). In addition, immunoblotting for LC3B confirmed an increase in the lipidated form of LC3B (LC3-II), which associates with the autophagosome membrane, in MT-hTER-47A-expressing cells (**Figure 2G**). Autophagic flux was also increased in MT-hTER-47A cells compared to vector and WT-hTER controls when cells were treated with the lysosomal protease inhibitors E64d and pepstatin A to block LC3-II turnover (**Figure 2G, Figure S2**). Overall, these results indicate that MT-hTER-47A-induced telomeric dysfunction is sufficient to induce both autophagy and senescence.

Figure 2

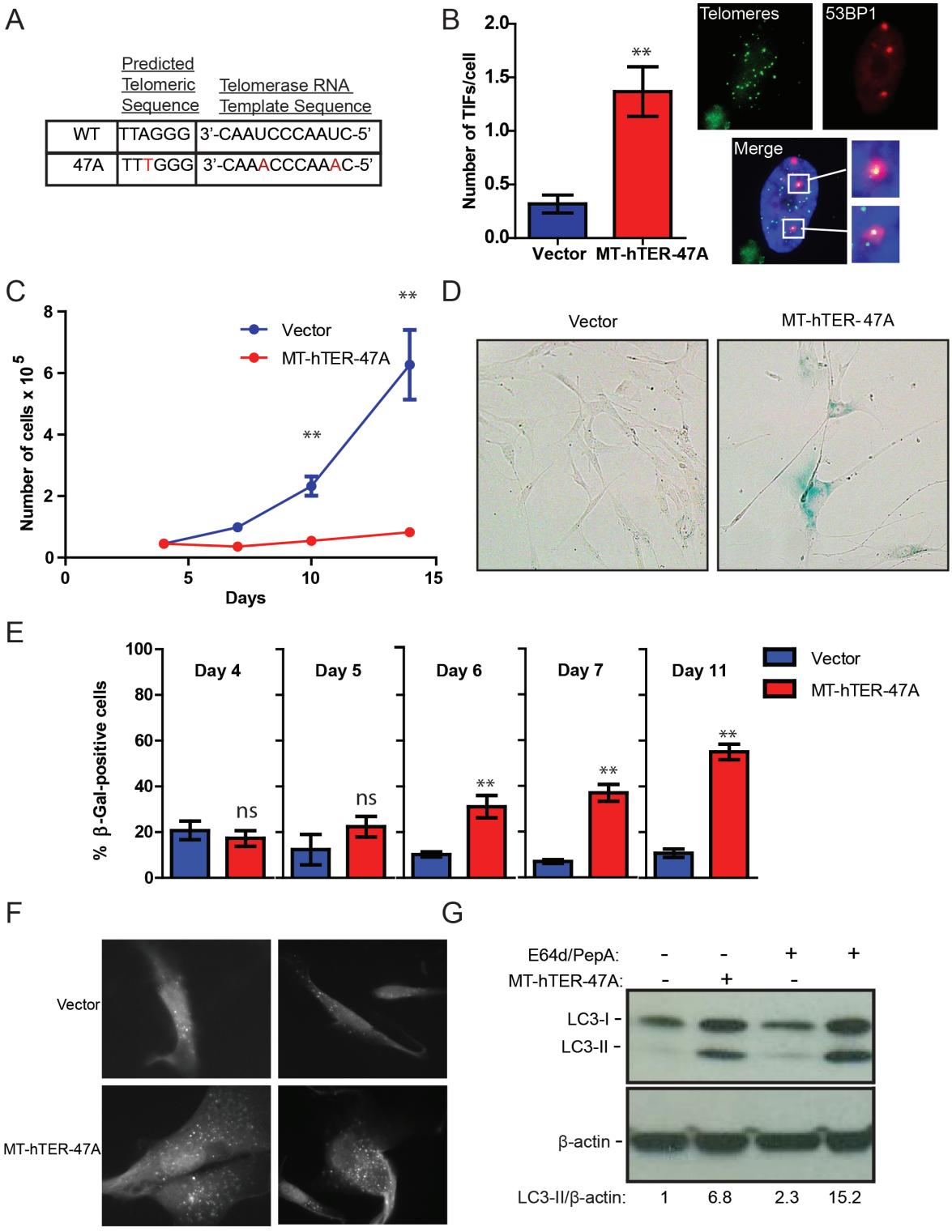
A
Predicted Telomeric Sequence
Telomerase RNA Template Sequence
WT
TTAGGG
3'-CAAUCCCAAUC-5'
47A
TTTGGG
3'-CAAACCCAAAC-5'
B
Number of TIFs/cell
Vector
MT-hTER-47A
Telomeres
53BP1
Merge
C
Number of cells x 10^5
Days
Vector
MT-hTER-47A
D
Vector
MT-hTER-47A
E
% β-Gal-positive cells
Day 4
Day 5
Day 6
Day 7
Day 11
ns
F
Vector
MT-hTER-47A
G
E64d/PepA:
MT-hTER-47A:
LC3-I
LC3-II
β-actin
LC3-II/β-actin: 1 6.8 2.3 15.2

Figure 2. Autophagy is induced in response to telomere dysfunction from MT-hTER-47A.

(**A**) Wild-type and MT-hTER-47A telomerase RNA template and predicted telomere repeat sequences. (**B**) Quantification of telomere dysfunction-induced foci (TIFs) and representative images 7 days after transduction with MT-hTER-47A or an empty vector. (**C**) Growth curve of control and MT-hTER-47A-treated WI-38-TERT fibroblasts. (**D**) Representative images of SA-β-Gal staining in vector or MT-hTER-47A-treated cells 7 days after transduction using a 20X objective. (**E**) Percentage of SA-β-Gal-positive cells at indicated times after MT-hTER-47A addition. (**F**) Two representative images of GFP-LC3B puncta for each condition 4 days after transduction with MT-hTER-47A or empty vector using a 100X objective. (**G**) LC3B immunoblot in control and MT-hTER-47A-transduced cell extracts in the presence or absence of the lysosomal protease inhibitors E64d and pepstatin A. Relative amounts of LC3-II are indicated below the blots. ** indicates significance at $P<0.01$ compared to empty vector control. Error bars in panels (**B and E**) represent standard error. Error bars in panel (**C**) represent standard deviation. Results are based on three or more parallel wells and are representative of at least 3 independent experiments.

Figure S2

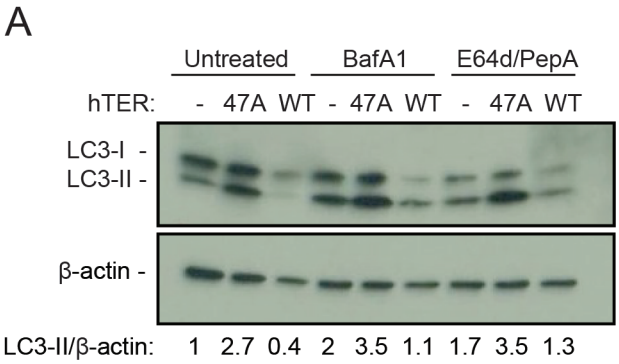

Figure S2. Autophagic flux is induced in response to MT-hTER compared to vector or WT-hTER.

(**A**) Immunoblot for LC3 in cells treated with WT or MT-hTER either in the presence or absence of the lysosomal inhibitors bafilomycin A_1, or E64d and pepstatin A.

Autophagy does not regulate the transition to TDIS.

Prior work implicates autophagy in promoting the transition to OIS (Andrew M. Leidal, 2012; Andrew R.J. Young, 2009) suggesting that the induction of autophagy we observed in response to telomeric dysfunction may similarly contribute to TDIS. To test this possibility, we used shRNAs targeting *ATG5* and *ATG7*, two proteins essential for the early steps of autophagosome formation (Noboru Mizushima, 2010). In WI-38-TERT cells, expression of these shRNAs reduced target mRNA and protein levels (**Figure S3**). Knockdown of *ATG5* or *ATG7* also resulted in a reduction in LC3-II formation following MT-hTER-47A treatment in the presence or absence of the lysosomal v-ATPase inhibitor bafilomycin A_1 ($BafA_1$) (**Figure 3A**), indicating that these shRNAs effectively block autophagy flux. In contrast to previous studies of OIS (Andrew M. Leidal, 2012; Andrew R.J. Young, 2009), MT-hTER-47A-induced TDIS was largely unaffected by inhibition of autophagy. The accumulation of SA-β-gal-positive cells after MT-hTER-47A treatment was not significantly affected by depletion of ATG5 or ATG7 (**Figure 3B, Figure S3**). Additionally, MKI67/Ki67 staining to identify cells actively engaged in the cell cycle did not show significant differences between autophagy-proficient and autophagy-deficient cells expressing MT-hTER-47A (**Figure 3C**). Lastly, autophagy inhibition did not affect the ability of WI-38 fibroblasts expressing MT-hTER-47A to grow in a colony-forming assay (**Figure 3D**). In fact, we observed fewer and smaller colonies of sh*ATG7*-treated cells in a colony-forming assay regardless of the addition of MT-hTER-47A. This data is consistent with previous results that autophagy inhibition alone may impair cell growth depending on the cell type and level of autophagy inhibition (Hyun Tae Kang, 2011).

Figure 3

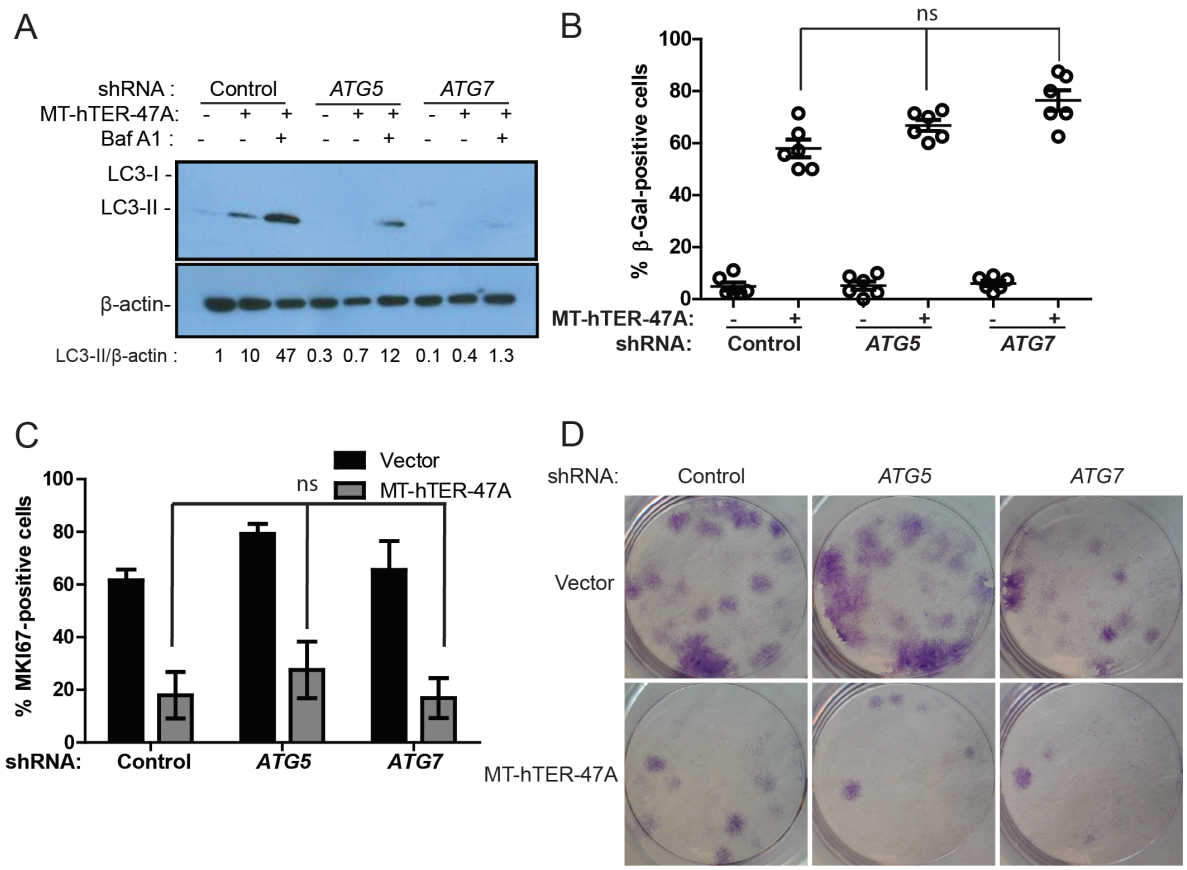
A
shRNA :
Control
ATG5
ATG7
MT-hTER-47A:
Baf A1 :
LC3-I -
LC3-II -
β-actin-
LC3-II/β-actin :
1 10 47 0.3 0.7 12 0.1 0.4 1.3
B
ns
% β-Gal-positive cells
MT-hTER-47A:
shRNA:
Control
ATG5
ATG7
C
Vector
MT-hTER-47A
ns
% MKI67-positive cells
shRNA:
Control
ATG5
ATG7
D
shRNA:
Control
ATG5
ATG7
Vector
MT-hTER-47A

Figure 3. Autophagy inhibition does not affect the senescence transition following MT-hTER-47A treatment of WI-38 fibroblasts.

(**A**) LC3B immunoblotting in WI-38-TERT fibroblasts transduced with a control, *ATG5*, or *ATG7* shRNA and treated with 25 nM $BafA_1$, 7 days after MT-hTER-47A addition. Relative amounts of LC3-II are indicated below the blots. (**B**) SA-β-gal staining 7 days after MT-hTER-47A addition. SA-β-gal staining showed a significant increase between vector and MT-hTER-47A cells ($P<0.05$) but no significant differences were observed between the MT-hTER-47A-treated samples. Error bars represent standard error. (**C**) MKI67 staining in WI-38-TERT fibroblasts expressing a control, *ATG5*, or *ATG7* shRNA, 7 days after MT-hTER-47A transduction. MT-hTER-47A-treated samples showed a significant depletion of MKI67-positive cells compared to controls ($P<0.05$). Error bars represent standard deviation. (**D**) Crystal violet-stained colonies showing colony forming efficiency upon platting $3x10^3$ cells 8 days after MT-hTER-47A addition. Results are representative of at least 3 independent experiments.

Figure S3

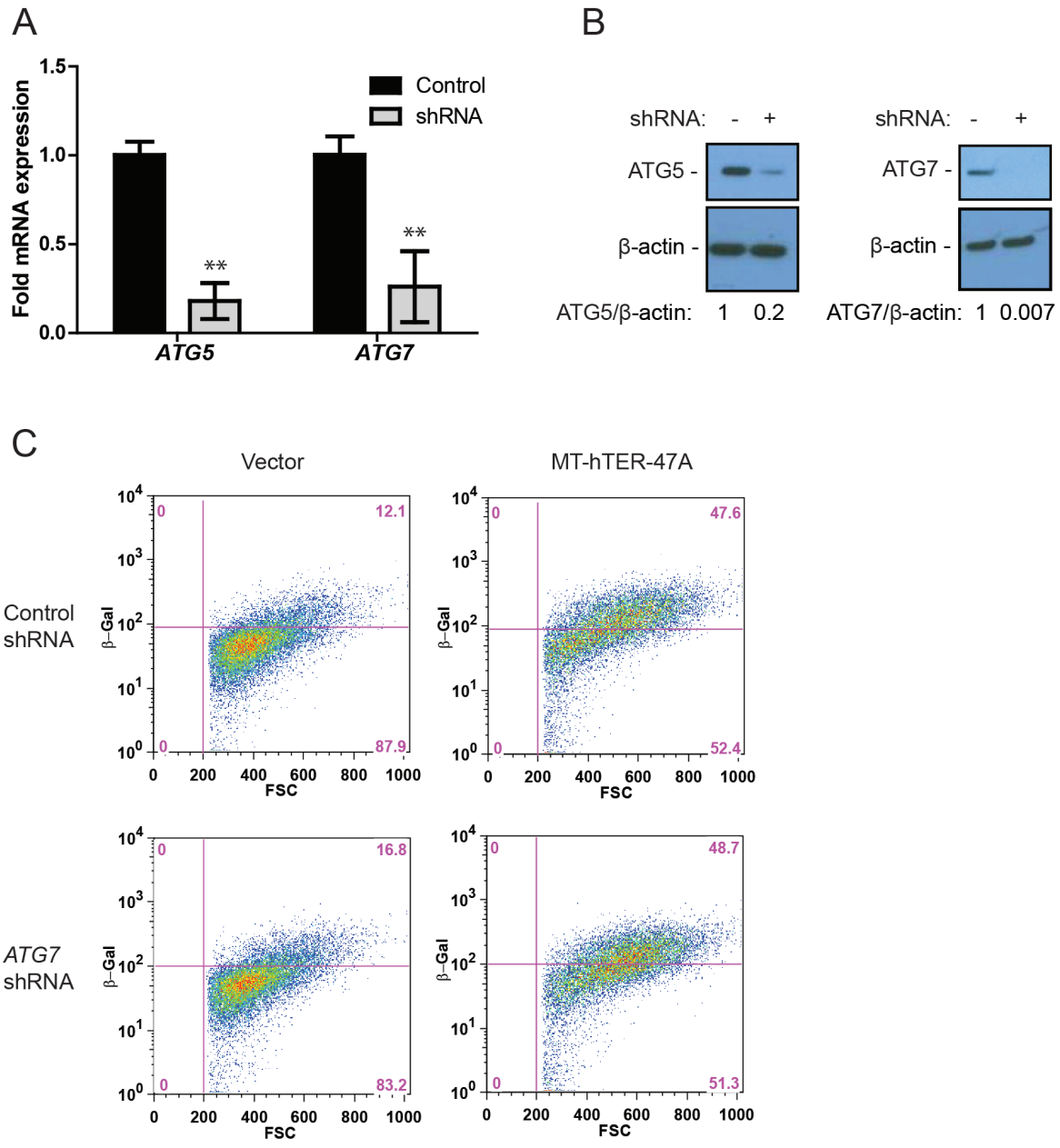
A
Fold mRNA expression
1.5
1.0
0.5
0.0
Control
shRNA
**
**
ATG5
ATG7
B
shRNA: - +
ATG5 -
β-actin -
ATG5/β-actin: 1 0.2
shRNA: - +
ATG7 -
β-actin -
ATG7/β-actin: 1 0.007
C
Vector
MT-hTER-47A
Control shRNA
ATG7 shRNA
β–Gal
FSC
12.1
87.9
47.6
52.4
16.8
83.2
48.7
51.3

Figure S3. Autophagy inhibition does not affect MT-hTER-induced senescence in WI-38 fibroblasts.

(**A**) Levels of *ATG5* and *ATG7* mRNA knockdown relative to control shRNA. (**B**) Immunoblot for ATG5 and ATG7 upon shRNA knockdown. (**C**) SA-β-Gal staining in autophagy proficient (control shRNA) or autophagy deficient (*ATG7* shRNA) WI-38 fibroblasts assayed by flow cytometry. Numbers indicate percent of cells occupying the indicated quadrant. SA-β-Gal-positive cells are located in the top right quadrant. **indicates significance at $P<0.01$. Error bars indicate standard deviation.

Previous studies of autophagy in OIS have predominantly utilized BJ fibroblasts (Andrew M. Leidal, 2012; Andrew R.J. Young, 2009; Jean-Philippe Coppé, 2008; Raffaella Di Micco, 2006). In contrast to WI-38 fibroblasts, senescence in BJ fibroblasts can be reversed upon inhibition of TP53/p53, likely due to differences in CDKN2A/p16 expression between these two cell types (Christian M. Beauséjour, 2003). We therefore tested whether autophagy inhibition alters the progression of TDIS in BJ-TERT fibroblasts. Despite robust depletion of *ATG5* and *ATG7* mRNA and protein as well as effective inhibition of induced autophagic flux (**Figure 4A, Figure S4**), the accumulation of SA-β-gal-positive cells following MT-hTER-47A treatment in BJ fibroblasts was unaffected (**Figure 4B**). Similarly, autophagy inhibition did not affect the ability of MT-hTER-47A-treated BJ fibroblasts to grow in a colony-forming assay (**Figure 4C**). Together, these data argue that autophagy does not play a significant role in MT-hTER-47A-induced senescence in human fibroblast cell lines.

Figure 4

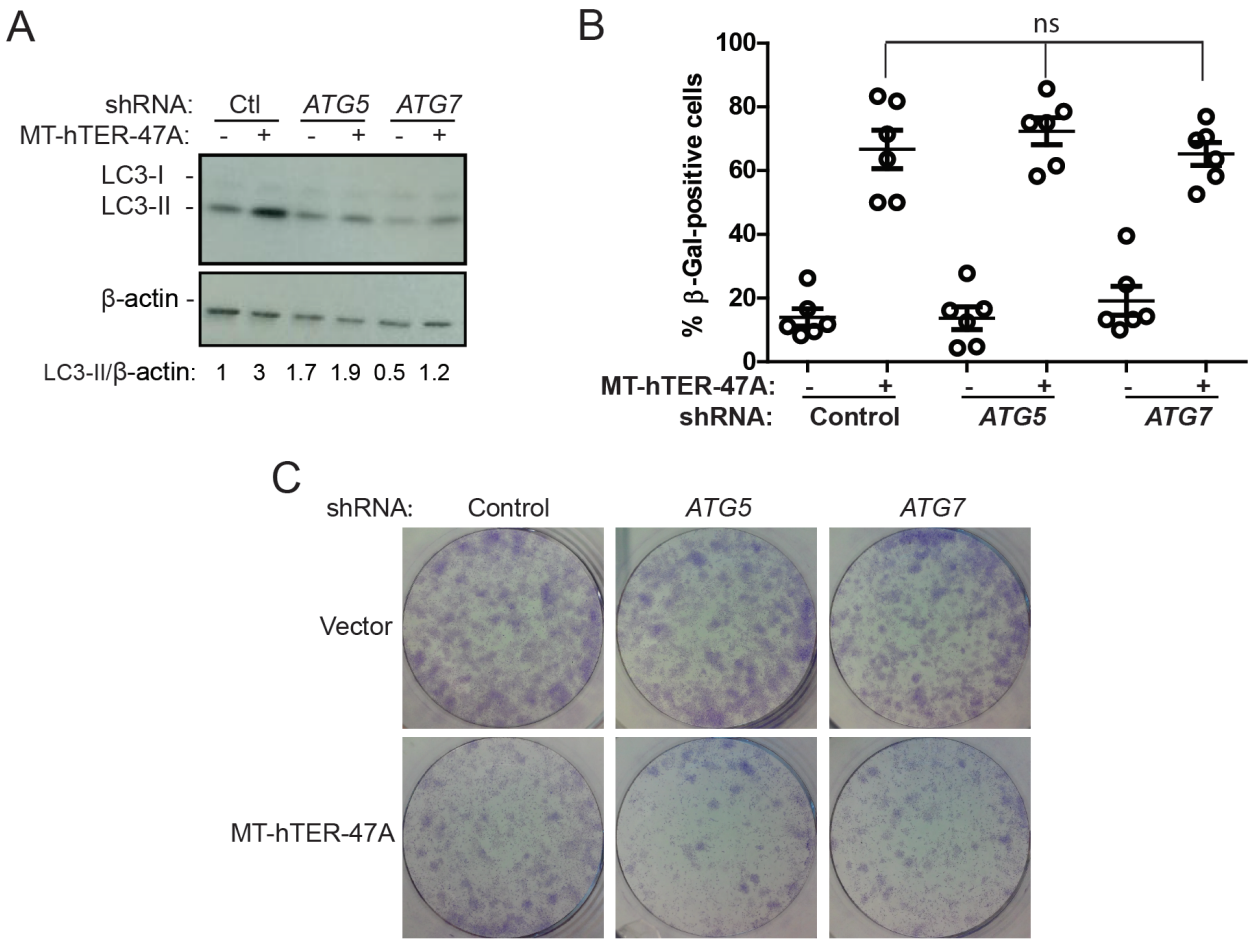
A
shRNA: Ctl ATG5 ATG7
MT-hTER-47A: - + - + - +
LC3-I -
LC3-II -
β-actin -
LC3-II/β-actin: 1 3 1.7 1.9 0.5 1.2
B
ns
% β-Gal-positive cells
100
80
60
40
20
0
MT-hTER-47A: - + - + - +
shRNA: Control ATG5 ATG7
C
shRNA: Control ATG5 ATG7
Vector
MT-hTER-47A

Figure 4. Autophagy inhibition does not affect the senescence transition following MT-hTER-47A treatment of BJ fibroblasts.

(**A**) LC3B immunoblotting in BJ-TERT fibroblasts transduced with a control, *ATG5*, or *ATG7* shRNA 7 days after MT-hTER-47A addition. Relative amounts of LC3-II are indicated below the blots. (**B**) SA-β-gal staining 7 days after MT-hTER-47A addition. SA-β-gal staining showed a significant increase between vector and MT-hTER-47A cells ($P<0.05$) but no significant differences were observed between the MT-hTER-47A-treated samples. Error bars represent standard error. (**C**) Crystal violet-stained colonies showing colony forming efficiency upon plating $3x10^3$ cells at day 8 after MT-hTER-47A addition. Data is representative of at least 3 independent experiments.

Figure S4

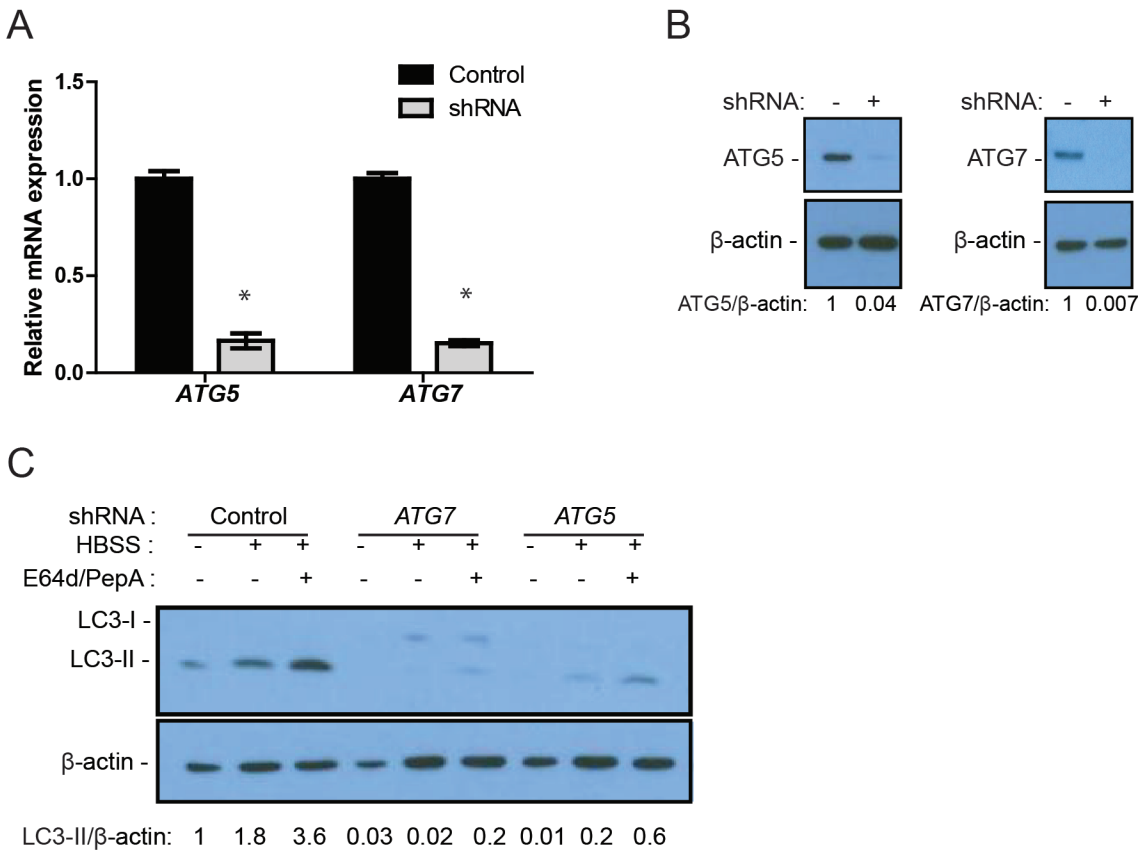

Figure S4. shRNA-mediated *ATG* silencing in BJ fibroblasts.

(**A**) Levels of *ATG5* and *ATG7* mRNA knockdown relative to control shRNA. (**B**) Immunoblot for ATG5 and ATG7 upon shRNA knockdown. (**C**) Immunoblot for LC3 in autophagy-proficient (Control shRNA) or autophagy-deficient (*ATG5* or *ATG7* shRNA) BJ fibroblasts upon nutrient starvation in the presence or absence of the lysosomal inhibitors E64d and pepstatin A. *indicates significance at $P<0.05$. Error bars indicate standard deviation.

The transition to TDIS occurs in the absence of a robust SASP.

Previous work suggests that autophagy supports the SASP during the transition to OIS, and autophagy inhibition slows the transition to OIS by delaying SASP induction (Andrew M. Leidal, 2012; Andrew R.J. Young, 2009; Masako Narita, 2011). Because the SASP reinforces senescence in an autocrine and paracrine fashion (Jean-Philippe Coppé, 2008; Juan Carlos Acosta, 2013; Thomas Kuilman, 2008), we reasoned that MT-hTER-47A-induced TDIS may be less dependent on autophagy induction than OIS due to a difference in the SASP between the two types of senescence. Notably, previous work has shown that the SASP from replicative senescent cells is reduced in overall magnitude compared to that produced from OIS (Jean-Philippe Coppé, 2008). To test this possibility in our system, we further scrutinized how MT-hTER-47A-induced SASP differs from that induced by the v-cyclin oncogene. We first confirmed that v-cyclin expression (**Figure 5A**) elicited high levels of senescence in BJ fibroblasts, as shown by the progressive accumulation of SA-β-gal-positive cells (**Figure 5B**). Importantly, similar numbers of senescent cells were observed in response to MT-hTER-47A and v-cyclin expression during the transition to senescence (**Figure 5B**). Next, we monitored the secretion of SASP factors during the transition to senescence. Since autophagy has been linked to the efficient synthesis and secretion of IL6 and IL8 during OIS, we focused on these two SASP cytokines in our studies (Andrew M. Leidal, 2012; Andrew R.J. Young, 2009; Masako Narita, 2011). In agreement with previous findings, v-cyclin overexpression induced rapid and robust secretion of both IL6 and IL8 during the transition to senescence (**Figure 5C and D**) (Andrew M. Leidal, 2012). In

contrast, the secretion of IL6 and IL8 was not significantly increased during this timeframe in the MT-hTER-47A-treated cells (**Figure 5C and D**).

To determine if this discrepancy was specific to MT-hTER-47A or was a common feature of telomere dysfunction-induced senescence, we induced telomere dysfunction in two other ways—by expressing another MT-hTER (MT-hTER-AU5) or an shRNA targeting *TIN2*, a member of the shelterin complex (**Figure S5**). These other forms of telomere dysfunction also induced autophagic flux and senescence (**Figure S5**). However, whereas v-cyclin-induced senescence was associated with a robust SASP during the period of senescence transition, TDIS induced by MT-hTER-AU5 or *TIN2* knockdown occurred in the absence of a robust induction of secreted IL6 or IL8, similar to what was seen with MT-hTER-47A (**Figure S5**).

Thus, both IL6 and IL8 production are much more limited in several models of TDIS compared to v-cyclin-induced OIS during the period of senescence transition. Despite these profound differences in the elaboration of these key SASP factors, BJ fibroblasts exhibit comparable levels of senescence in response to either telomeric dysfunction or v-cyclin expression during the period of senescence transition (**Figure 5B, Figure S5**).

Figure 5

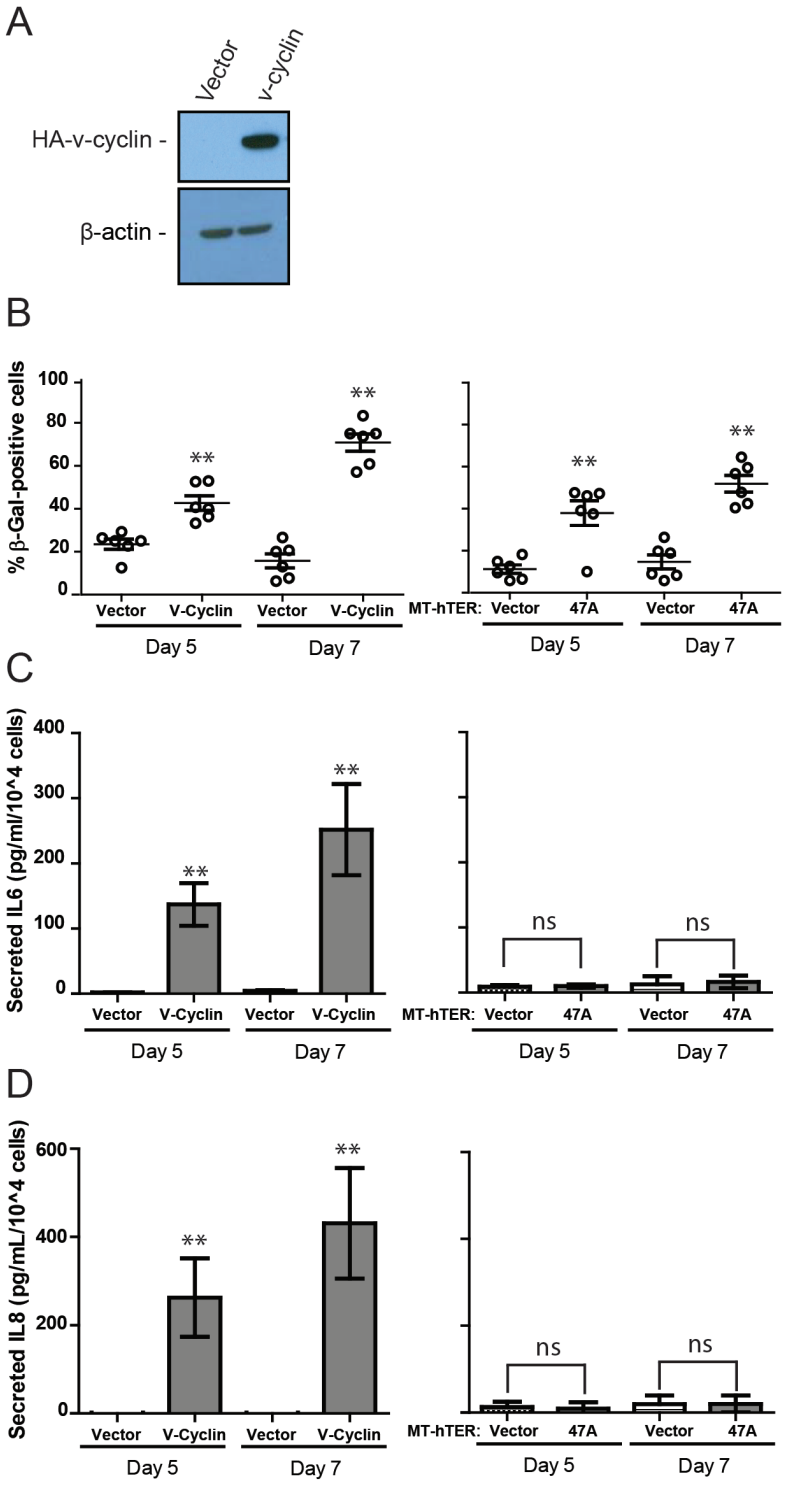
A
Vector
v-cyclin
HA-v-cyclin -
β-actin -
B
% β-Gal-positive cells
100
80
60
40
20
0
**
Vector
V-Cyclin
Day 5
Day 7
MT-hTER:
47A
C
Secreted IL6 (pg/ml/10^4 cells)
400
300
200
100
ns
D
Secreted IL8 (pg/mL/10^4 cells)
600

Figure 5. Senescence transition in the absence of a robust SASP in MT-hTER-47A-expressing BJ fibroblasts.

(**A**) Immunoblot for HA to detect overexpressed HA-v-cyclin protein in BJ fibroblasts 7 days after transduction. (**B**) SA-β-gal staining during the period of senescence transition—5 and 7 days after MT-hTER-47A or HA-v-cyclin addition—in BJ-TERT fibroblasts. Error bars represent standard error. (**C**) IL6 and (**D**) IL8 Elisa from conditioned media harvested from BJ-TERT fibroblasts at various time points after MT-hTER-47A or HA-v-cyclin addition. Error bars represent standard deviation. Elisa data includes 2 independent experiments. SA-β-Gal data is representative of at least 3 independent experiments. ** indicates significance at $P<0.01$ when compared to the vector control.

Figure S5

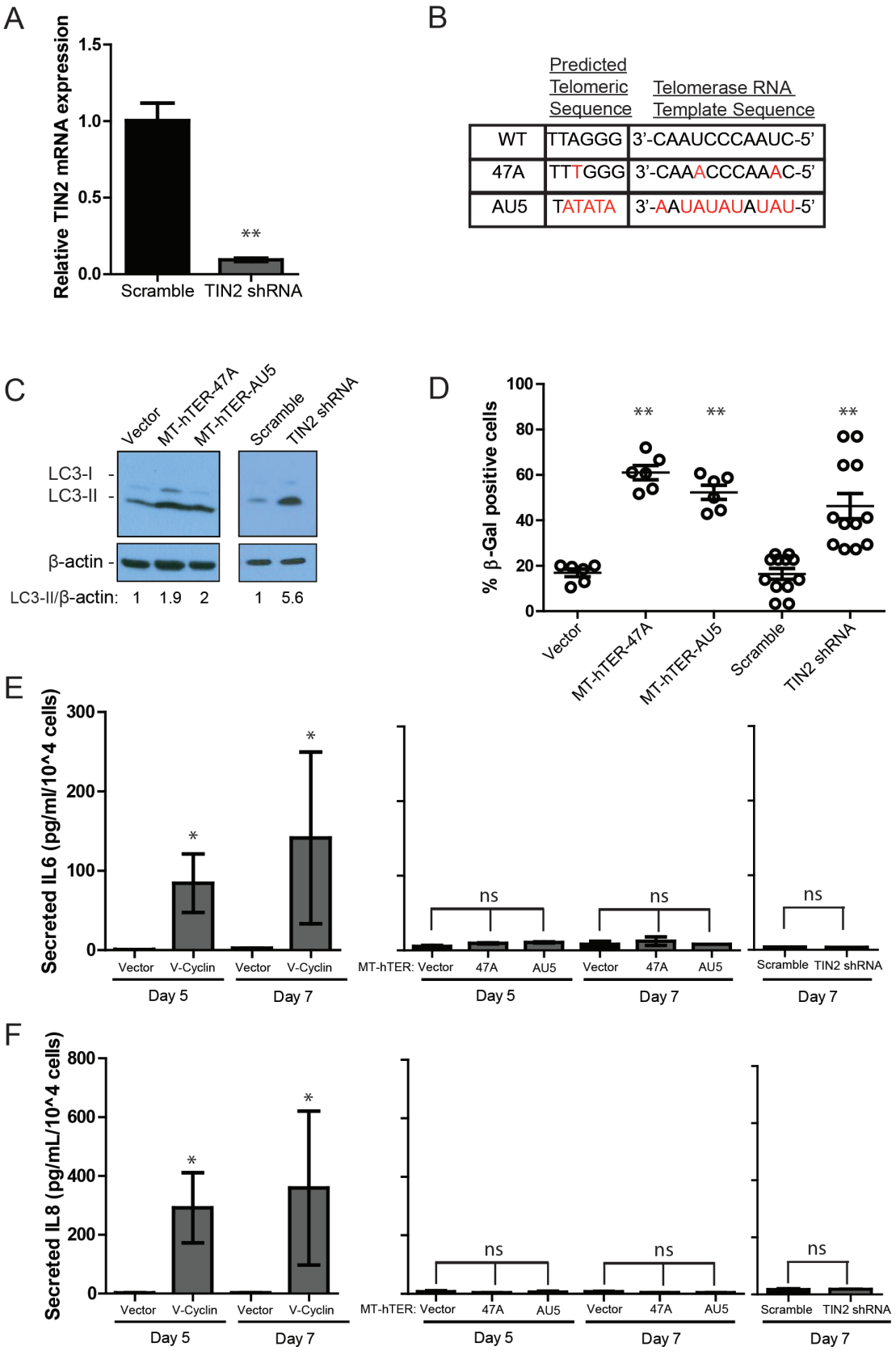
A
Relative TIN2 mRNA expression
1.5
1.0
0.5
0.0
**
Scramble
TIN2 shRNA
B
Predicted Telomeric Sequence
Telomerase RNA Template Sequence
WT TTAGGG 3'-CAAUCCCAAUC-5'
47A TTTGGG 3'-CAAACCCAAAC-5'
AU5 TATATA 3'-AAUAUAUAUAU-5'
C
Vector
MT-hTER-47A
MT-hTER-AU5
Scramble
TIN2 shRNA
LC3-I
LC3-II
β-actin
LC3-II/β-actin: 1 1.9 2 1 5.6
D
% β-Gal positive cells
100
80
60
40
20
0
**
**
**
Vector
MT-hTER-47A
MT-hTER-AU5
Scramble
TIN2 shRNA
E
Secreted IL6 (pg/ml/10^4 cells)
300
200
100
0
*
*
Vector
V-Cyclin
Vector
V-Cyclin
Day 5
Day 7
ns
ns
ns
MT-hTER: Vector
47A
AU5
Vector
47A
AU5
Day 5
Day 7
Scramble
TIN2 shRNA
Day 7
F
Secreted IL8 (pg/mL/10^4 cells)
800
600
400
200
0
*
*
Vector
V-Cyclin
Vector
V-Cyclin
Day 5
Day 7
ns
ns
ns
MT-hTER: Vector
47A
AU5
Vector
47A
AU5
Day 5
Day 7
Scramble
TIN2 shRNA
Day 7

Figure S5. Senescence transition in the absence of a robust SASP is a common feature of several forms of TDIS in BJ-TERT fibroblasts.

(**A**) Quantitative RT-PCR for *TIN2* transcript to confirm effective knockdown with the *TIN2* shRNA. (**B**) Wild-type, MT-hTER-47A, and MT-hTER-AU5 telomerase RNA template and predicted telomere repeat sequences. (**C**) Immunoblotting for LC3B to detect autophagy induction upon telomere dysfunction. (**D**) SA-β-gal staining during the period of senescence transition—7 days after MT-hTER or HA-v-cyclin addition. Error bars represent standard error. (**E**) IL6 and (**F**) IL8 Elisa from conditioned media harvested from BJ-TERT fibroblasts at various time points after MT-hTER, *TIN2* shRNA, or HA-v-cyclin addition. Except when specified, error bars represent standard deviation. * indicates significance at $P<0.05$ when compared to control. ** indicates significance at $P<0.01$ when compared to the vector control. Data is representative of at least 2 independent experiments.

TDIS and OIS exhibit different levels of DNA damage.

Previous studies have identified the requirement for persistent DNA damage signaling, in part through the ATM pathway, for the development of the SASP (Francis Rodier, 2009). However, no study has thoroughly examined the correlation between levels of DNA damage and magnitude of the SASP.

We reasoned that the differences in the SASP between OIS and several forms of TDIS might be due to differences in the levels of DNA damage triggered by oncogene overexpression and telomere dysfunction. To test this, we performed fluorescent in situ hybridization to label telomeres combined with immunofluorescence to visualize 53BP1 protein, which accumulates at sites of DNA damage. Interestingly, we found that v-cyclin expression led to nearly 4-fold more DNA damage foci per cell compared to two different forms of telomere dysfunction—MT-hTER-47A and loss of TIN2—(**Figure 6A**). As expected, v-cyclin-induced DNA damage was almost entirely non-telomeric while telomere dysfunction-induced DNA damage was predominantly telomeric (**Figure 6B**).

We also assessed DNA damage by immunoblotting for phosphorylated ATM (Ser1981) and p53 (Ser15). In response to DNA damage, ATM autophosphorylation on Serine 1981 contributes to its activation. When ATM is fully activated, it phosphorylates p53 at Serine 15, releasing it from MDM2 inhibition and activating downstream DNA damage signaling pathways and DNA repair. Phosphorylation of p53 at Serine 15 and ATM at Serine 1981 are markers of DNA damage signaling. In our system, telomere dysfunction or overexpression of the v-cyclin oncogene caused phosphorylated ATM and p53 to accumulate (**Figure 6C to D**). However, cells overexpressing v-cyclin

accumulated phosphorylated ATM and p53 to a greater extent than cells expressing MT-hTER-47A, MT-hTER-AU5, or an shRNA targeting *TIN2* (**Figure 6C to D**).

While both telomere dysfunction and v-cyclin expression led to comparable levels of senescence during the period of senescence transition (**Figure 5B, Figure S5**), cells expressing v-cyclin exhibited a more robust DNA damage phenotype than those experiencing telomere dysfunction. This considerable difference in the levels of DNA damage signaling between these two forms of senescence may lead to differences in downstream events that may guide the functions of the senescent cell.

Figure 6

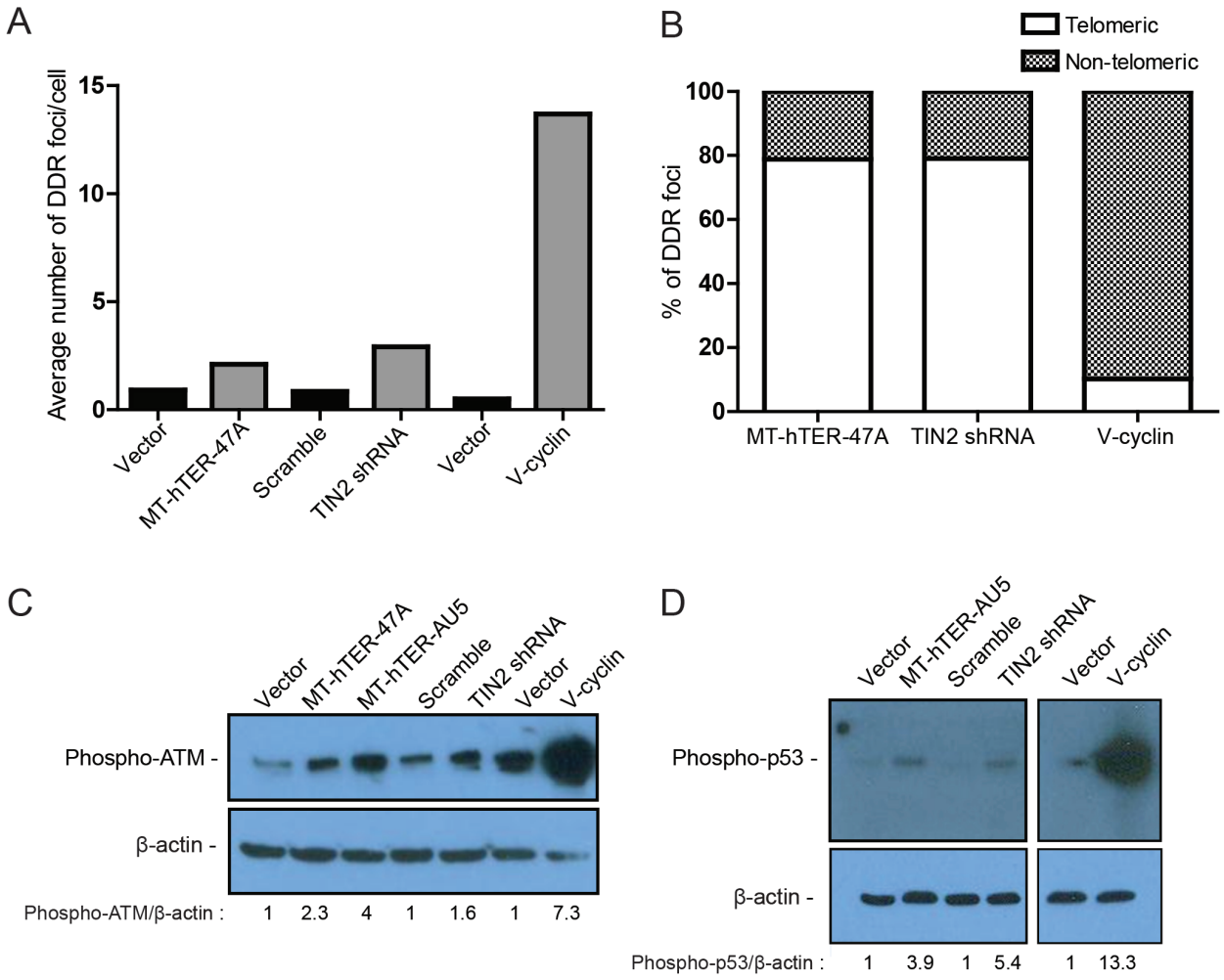
A
Average number of DDR foci/cell
15
10
5
0
Vector
MT-hTER-47A
Scramble
TIN2 shRNA
Vector
V-cyclin
B
Telomeric
Non-telomeric
% of DDR foci
100
80
60
40
20
0
MT-hTER-47A
TIN2 shRNA
V-cyclin
C
Vector
MT-hTER-47A
MT-hTER-AU5
Scramble
TIN2 shRNA
Vector
V-cyclin
Phospho-ATM -
β-actin -
Phospho-ATM/β-actin : 1 2.3 4 1 1.6 1 7.3
D
Vector
MT-hTER-AU5
Scramble
TIN2 shRNA
Vector
V-cyclin
Phospho-p53 -
β-actin -
Phospho-p53/β-actin : 1 3.9 1 5.4 1 13.3

Figure 6. Cells expressing the v-cyclin oncogene have higher levels of DNA damage than those with telomere dysfunction.

(**A**) Number of DNA damage response (DDR) foci per cell upon treatment with MT-hTER, or v-cyclin. (**B**) Quantification of TIFs to measure the colocalization of DDR foci with telomeres in cells treated with MT-hTER or v-cyclin. (**C**) Immunoblotting for phosphorylated ATM (Ser1981) in cells treated for 8 days with MT-hTER, *TIN2* shRNA or v-cyclin. Band intensities normalized to the appropriate vector or scramble control are located below the immunoblot. (**D**) Immunoblotting for phosphorylated p53 (Ser15) in cells treated for 8 days with MT-hTER, *TIN2* shRNA, or v-cyclin. The blot was cut to produce this figure—each half of the blot originated from the same gel and exposure. Band intensities normalized to the appropriate vector or scramble control are located below the immunoblot. Data is representative of at least 3 independent experiments.

High levels of DNA damage correlate with the elaboration of a more robust SASP during transition to senescence.

Because we observed significantly higher levels of both DNA damage and secreted SASP factors in response to v-cyclin when compared to telomere dysfunction, we reasoned that DNA damage levels may correlate with SASP levels during the period of senescence transition. To test this, we expressed v-cyclin in BJ-TERT fibroblasts and performed flow cytometry to measure levels of phosphorylated ATM, phosphorylated p53, and intracellular IL6 at the single-cell level during the early stages of senescence development—3 days after v-cyclin expression.

In preliminary data, there was only a weak correlation between levels of phosphorylated ATM and phosphorylated p53 (R square=0.08) (data not shown). When assessing the correlation between DNA damage markers and IL6 levels, we found a threshold of intracellular IL6 above which IL6 and phosphorylated-ATM were positively correlated (R square=0.35) (**Figure 7A**). Below this threshold, there was no correlation between levels of IL6 and phosphorylated-ATM (R-square=0.05) in v-cyclin-expressing cells. Among vector-treated cells, few displayed IL6 levels above the threshold identified and there was no correlation between levels of IL6 and phosphorylated ATM (R square=0.002) (**Figure 7A**). Surprisingly, we did not find a threshold of IL6 above which levels of phosphorylated-p53 correlated with levels of IL6. Instead, there seemed to be no correlation between IL6 and phosphorylated-p53 in our system (R square=0.004) (**Figure 7B**). Due to the preliminary nature of this data, replicate experiments will have to be performed before robust conclusions can be drawn from these results.

Together, these data argue that during early stages of senescence, cells expressing high levels of IL6 also exhibit high levels of phosphorylated ATM, but not phosphorylated p53. This interesting discrepancy may be explained by the fact that p53 impairs development of the SASP (Jean-Philippe Coppé, 2008). However, further experimentation will have to be conducted to validate these results utilizing various forms of senescence inducers, including DNA damaging agents, and other oncogenes.

Figure 7

A

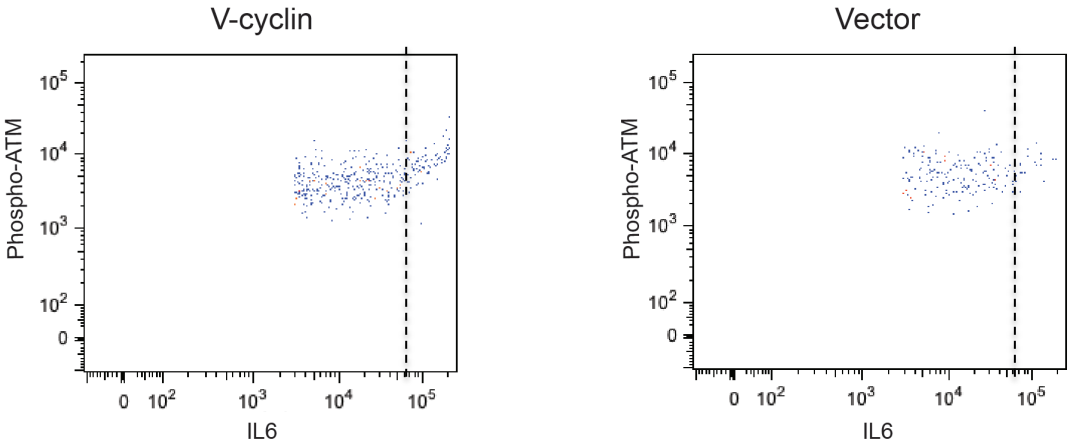
V-cyclin
Vector
Phospho-ATM
IL6
0
10^2
10^3
10^4
10^5

B

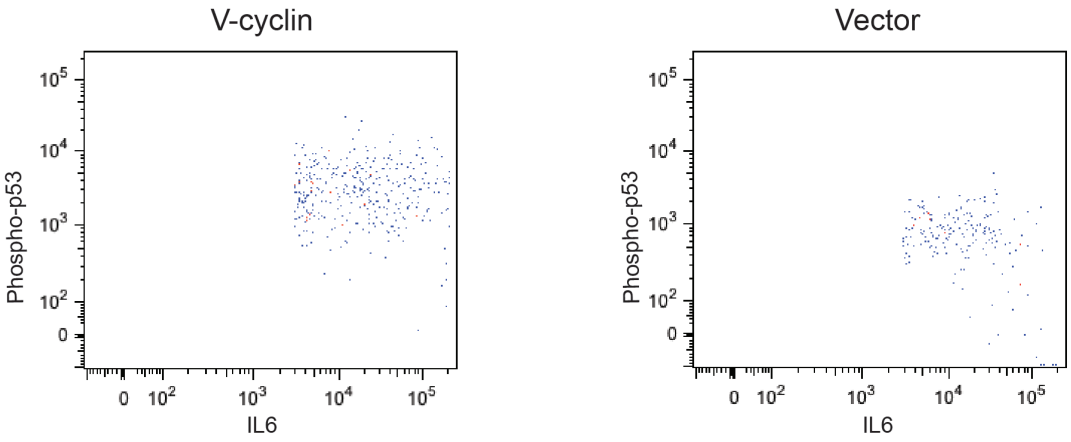
V-cyclin
Vector
Phospho-p53
IL6
0
10^2
10^3
10^4
10^5

Figure 7. Levels of DNA damage positively correlate with levels of secreted IL6 and IL8 during early senescence.

(**A**) Flow cytometry of vector or v-cyclin-expressing cells 3 days after transduction, stained for intracellular IL6 and phosphorylated-ATM (Ser1981). The dashed line represents the threshold of IL6 above which levels of phosphorylated-ATM are positively correlated with levels of IL6. (**B**) Flow cytometry of vector or v-cyclin-expressing cells 3 days after transduction, stained for intracellular IL6 and phosphorylated-p53 (Ser15). Data is representative of 1 experiment.

MATERIALS AND METHODS

Cell culture

Human BJ and WI-38 fibroblasts were obtained from ATCC and immortalized by retroviral expression of TERT. HMECs were grown in mammary epithelial growth medium (MEGM) supplemented with hEGF, hydrocortisone, and insulin (Lonza, CC-2551, CC-3151, CC-3150). All other cells were cultured in Dulbecco modified Eagle medium medium (Invitrogen, 11965) supplemented with 10% FBS. All cells were grown at 37 ^{o}C in 5% CO2. For viral transduction, cells were infected for 24 h with lentivirus or 48 h with retrovirus, and antibiotic selection was started 24 h after virus removal at the following concentrations: puromycin (Life Technologies, A11138-02) at 1.5 ug/mL for 2 to 3 days, or blasticidin (Life Technologies, A11139-03) at 8 ug/mL for 3 days. For the pSMB retroviruses expressing control, *ATG5*, or *ATG7* shRNAs, BJ and WI-38 fibroblasts were infected for 8 h followed by a second 24-h infection.

Plasmids and viruses

The TER-expressing lentivector included a wild-type or mutant TER gene driven by the *IU1* promoter and a puromycin resistance gene driven by the *CMV* promoter (Shang Li, 2004). The pSMB retroviral vectors expressing shRNAs against *ATG5* or *ATG7*, as well as the retroviral HA-v-cyclin pBMN plasmid, were a gift from Andrew Leidal (Dalhousie University). The shRNA against *TIN2* was a gift from Beth Cimini (UCSF). The shRNA targeting sequences for autophagy inhibition were as follows: 5'-ATCTCGCTTGGGCGAGAGTAAG-3' (nontargeted control); 5'-

CTTTGATAATGAACAGTGAGA-3' (*ATG5*); 5'-GGAGTCACAGCTCTTCCTTAC-3' (*ATG7*). The shRNA targeted sequences for knockdown of *TIN2* were as follows: 5'-GTTCTACAACGTAACGAGGTT-3' (nontargeted control); 5'-GCAAGGAAGAACATGCGATATA-3' *(TIN2).* The retroviral pBABE GFP-LC3B plasmid has been previously described and is available through AddGene (22405) (Christopher Fung, 2008). Lentiviruses and retroviruses were produced as previously described (Bradley A. Stohr, 2010).

Cell proliferation, colony formation, SA- β-gal assays

Growth curves were carried out by plating 4.5 x 10^4 cells per well of a 6-well plate and counting cell number by hemocytometer every 3 days, which is defined as one passage. SA-β-gal was measured according to manufacturer's instructions (Sigma-Aldrich, G5635). Six fields from 3 separate wells were analyzed for each of 3 independent experiments. Flow cytometry detection of SA- β-gal was performed as previously described (Florence Debacq-Chainiaux, 2009). Briefly, cells were treated for 1 h with 100 nM $BafA_1$ (Sigma-Aldrich, B1793) followed by addition of 33 uM C_{12}FDG (Life Technologies, D2893) for 1.5 h and analysis using a BD FACS Calibur instrument (2100 Derry Rd. W., Suite 100 Mississauga, ON L5N OB3). To examine colony formation, 3 x 10^3 cells were plated in each well of a 6-well plate in triplicate 7 or 8 days after infection with MT-hTER-47A-expressing lentivirus. Colonies were fixed and stained with 0.05% crystal violet (Sigma, C3886) 9 days (BJ fibroblasts) or 14 to 18 days (WI-38 fibroblasts) after plating. Washed and dried plates representative of 3 independent experiments were imaged.

Immunofluorescence and fluorescent in situ hybridization (FISH)

Cells were seeded on coverslips and fixed with 4% paraformaldehyde (Electron Microscopy Services, 15710) for 10 min. After permeabilization with 0.5% NP-40 (Sigma, 18896), cells were blocked in PBG (0.2% (w/v) gelatin from cold water fish skin (Sigma, G7765), 0.5% (w/v) bovine serum albumin (Sigma, A2153) in 1X phosphate-buffered saline) and incubated overnight with a 1:100 dilution of MKI67/Ki67 antibody (Millipore, AB9260), or a 1:500 dilution of 53BP1 antibody (Novus Biologicals, NB100-304). To visualize TIFs, the 53BP1-labeled cells were further treated with ethanol dehydration, followed by incubation for 2-3 hours in hybridization mix (70% formamide, 1% blocking buffer, 10mM Tris HCl, pH7.2, and PNA FISH probe TMR-OO-5′-$[CCCTAA]_3$-3′, Panagene). Cells were subsequently washed and dehydrated with ethanol as previously described (Morgan E. Diolaiti, 2013). All images were obtained using a Metasystems Metafer slide scanning platform (70 Bridge Street Suite 100, Newton, MA 02458) in conjunction with a Zeiss Axio Imager Z2 upright microscope (5160 Hacienda Dr., Dublin, CA 94568) using a Zeiss 63X 1.4 NA Plan APOCHROMAT lens (5160 Hacienda Dr., Dublin, CA 94568) and Metafer software.

Gene expression

For quantitative RT-PCR, RNA was harvested using an RNeasy extraction kit (Qiagen, 74104). 50 ng of RNA was used in a quantitative RT-PCR reaction using the Brilliant II SYBR Green One-Step QRT-PCR kit (Agilent Technologies, 600825). mRNA expression relative to B2M was determined by calculating 2^(- ΔΔCT). Primers used for amplification are listed in Table 1.

IL6 and IL8 ELISA

The concentration of secreted IL6 and IL8 was determined from 24-h conditioned full media harvested at the indicated time points using the R&D Quantikine Elisa kit (R&D Systems, D6050, D8000C). The data was normalized to cell number at the time of conditioned media harvest and reported as ng per 10^4 cells over the 24-h period. The ELISA data for IL6 and IL8 derive from two independent experiments, each of which included triplicate measurements.

Autophagy assays

To examine autophagy flux, cells were treated with a single dose of $BafA_1$ (25 nM) (Sigma-Aldrich, B1793) for 1 h, E64d (10 ug/mL) and pepstatin A (10 ug/mL) for 5 h, or a vehicle control (DMSO or 100% ethanol) (Sigma-Aldrich, P5318, 11707, Enzo-PI107) as previously described (Elsa-Noah N'Diaye, 2009; Rebecca Locka, 2011). For starvation assays, cells were washed 3 times with phosphate-buffered saline (PBS) (Life Technologies, 14190) followed by HBSS (Invitrogen-14170) treatment for 1 h.

Immunoblotting

Cells were lysed in RIPA buffer supplemented with a protease and phosphatase-inhibitor cocktail (Thermo Scientific, 78440). Protein concentrations were determined using a BCA protein assay kit (Thermo Scientific 23225). Samples were run on 4-20% Tris-glycine gels after dilution in 2X Laemmli sample buffer supplemented with beta-mercaptoethanol. Immunoblotting for LC3-II was performed with a 1:1000 dilution of LC3B antibody that has been previously described and is now commercially available

(EMD Millipore, ABC232) (Christopher Fung, 2008). Immunoblotting for ATG5 was performed using a 1:500 dilution of ATG5 antibody (Cell Signaling Technology, 2630). Immunoblotting for ATG7 was performed using a 1:100 dilution of ATG7 antibody (Santa Cruz Biotechnology, sc-8668). Immunoblotting for HA-v-cyclin was performed using a 1:1000 dilution of HA antibody (Covance, MMS-101P). Immunoblotting for β-actin was performed using a 1:30,000 dilution of β-actin-HRP antibody (Abcam, ab20272). Immunoblotting for phosphorylated-ATM (S1981) was performed using a 1:500 dilution of phosphor-ATM (S1981) antibody (Rockland, 200-301-400). Immunoblotting for phosphorylated-p53 (Ser15) was performed using a 1:500 dilution of phospho-p53 antibody (Cell Signaling Technology, 9284). To quantify bands, Fiji software was used to measure band intensity of the protein of interest divided by the band intensity of β-actin.

Flow Cytometry

Flow cytometry for phosphorylated-p53, phosphorylated-ATM, and IL6 was performed as previously described with a few modifications (Peter Krutzik, 2003). Briefly, cells were harvested and washed in PBS before being fixed in 2% PFA for 15 minutes on ice. After washing in PBS, cells were resuspended in 100% MeOH and stored at -80^{o}C until processing (1-2 weeks). At the time of processing for flow cytometry, MeOH was removed by centrifugation and cells were washed twice in PBS, followed by a wash in flow buffer (2% BSA in PBS with 2uM EDTA). Antibody incubations were performed in 100uL of flow buffer at the following concentrations: 5ug/mL of phosphorylated-ATM (S1981) (Rockland, 200-301-400), 1ug/mL of goat anti-mouse FITC (Invitrogen, A-

11001), 4ug/mL of phosphorylated-p53 conjugated to APC (Ser15) (Cell Signaling, 8695), 2ug/mL of IL6 conjugated to PE (BD Biosciences, 554545). Isotype control antibody incubations were performed at the following concentrations: 5ug/mL of mouse antibody, 4ug/mL of mouse-IgG1-APC isotype antibody, 2ug/mL of mouse-IgG1-PE isotype antibody. All flow cytometry was performed on a BD Fortessa flow cytometer. Analysis of flow cytometry data was done using Flowjo (Treestar).

Statistics

Data for ELISAs, growth curves, SA- β-gal analysis, and MKI67 staining was performed using a One-Way ANOVA, followed by pairwise Student t tests with a Holm-Sidak correction for multiple comparisons. All statistical tests were done using R. Data was plotted using GraphPad Prism.

Table 1. Primers used for quantitative RT-PCR analysis

Target	**Forward Primer**	**Reverse Primer**
B2M	TCACGTCATCCAGCAGAGAAATGGA	CACACGGCAGGCATACTCATCTTT
ATG5	TGTTTCGTCCTGTGGCTG	GCAGAGGTGTTTCCAACATTG
ATG7	GCAGTTTCCAGTCTGTTGAAG	CTTTTCCCATCCAACTGCTTTAG
TIN2	GCGGCTAGCTGGCAGGTTGT	CAGCGCGCAGAGATCGCAGA

ACKNOWLEDGEMENTS

Grant support includes the NIH (K08 CA134552 to BAS, R01 CA188404 to JD) and American Cancer Society IRG-97-150-14 to BAS. This material is based upon work supported by the National Science Foundation under Grant No. 1144247 to FAM. Special thanks to Miranda Broz for her help conducting the flow cytometry experiments. We would also like to thank Beth Cimini, Drs. Amir Goldkorn, and Andrew Leidal for providing research materials.

CHAPTER 3

Genome instability driven by targeted telomere dysfunction is autophagy-independent

Content in this chapter was modified from the following publication:

Mar, FA, Debnath, J., Stohr BA. (2015). Autophagy-independent senescence and genome instability driven by targeted telomere dysfunction. *Autophagy, 11*(3): 527-37

SUMMARY

Autophagy is required for controlling levels of key proteins involved in DNA damage signaling and repair pathways that contribute to the generation of chromosome fusions induced by telomere dysfunction. In this study, we interrogated the role of the autophagy pathway in the generation of chromosome fusions triggered by several forms of telomere dysfunction—MT-mTER-47A, and expression of a dominant negative form of the shelterin protein Tpp1. Whereas autophagy was readily induced by these two forms of telomere dysfunction, inhibition of autophagy did not affect the number of chromosome fusions. Overall, the data presented here highlights the autophagy-independent nature of DNA damage repair pathways induced by telomere dysfunction.

HIGHLIGHTS

- Autophagy is induced in mouse embryonic fibroblasts following two distinct forms of targeted telomere dysfunction.
- Complete ablation of autophagy has no impact on chromosome fusions triggered by telomere dysfunction.

RESULTS

Autophagy does not influence telomere dysfunction-induced chromosome fusions.

In addition to inducing senescence, telomere dysfunction causes genomic instability primarily through the production of chromosome fusions, which occur upon recognition of the de-protected chromosome ends by the DNA damage repair machinery (Wilhelm Palm, 2008). In an attempt to "repair" the exposed chromosome ends, the DNA repair machinery fuses chromosomes together through classical or alternative nonhomologous end joining (C-NHEJ and A-NHEJ, respectively) (Rekha Rai, 2010). Telomere dysfunction-induced fusions can then drive further instability through iterative breakage-fusion-bridge cycles during subsequent mitoses (Murnane, 2012).

Given the ability of autophagy to modulate DNA repair (Praveen Rajendran, 2013; Robert T, 2011), we sought to determine if autophagy influences the rate or pattern of telomere dysfunction-induced chromosome fusions. Such fusions are challenging to study in primary human cells with intact checkpoints because telomere dysfunction induces rapid cell cycle arrest (Jan Karlseder, 2002). In contrast, because immortalized mouse embryonic fibroblasts (MEFs) do not exhibit cell cycle arrest in response to telomeric dysfunction, they are a well-established and highly useful model for the study of telomere dysfunction-induced genomic instability, including chromosome fusions (Rekha Rai, 2010; Wilhelm Palm, 2008). Therefore, to examine the role of the autophagy pathway in telomere dysfunction-induced chromosome fusions, we used mouse TERT-expressing immortalized MEFs from littermate *Atg5*$^{+/+}$ or *atg5*$^{-/-}$ mice and

littermate *Atg7*$^{+/+}$ or *atg7*$^{-/-}$ mice. We first induced telomere dysfunction by expressing MT-mTER-47A in autophagy-proficient or autophagy-deficient immortalized MEFs. Autophagy was enhanced in response to MT-mTER-47A in autophagy-proficient MEFs following nutrient starvation with Hanks buffered salt solution (HBSS) and treatment with $BafA_1$ (**Figure 1A**). In addition, MT-mTER-47A treatment significantly induced chromosome fusions as monitored by metaphase analysis (**Figure 1B**). Importantly, the number of fusions did not significantly differ in the autophagy-proficient and autophagy-deficient cells, suggesting that autophagy did not influence the fusion process (**Figure 1C to D**).

Chromosome fusions induced by MT-mTER-47A are thought to arise predominately through ATM-dependent C-NHEJ (Bradley A. Stohr, 2008; Bradley A. Stohr, 2010). In contrast, fusions induced by overexpression of Tpp1$^{\Delta RD}$, a dominant-negative form of the telomeric shelterin component Tpp1, occur through A-NHEJ, a fundamentally different DNA repair mechanism (Rekha Rai, 2010). While C-NHEJ is ligase IV-dependent and usually occurs through ligation of blunt DNA ends, A-NHEJ typically requires 3' end processing and generates microhomology at the fusion point (Ludovic Deriano, 2013). Of note, the CtIP protein, which is reportedly regulated by autophagy, has been implicated in A-NHEJ and chromosome fusions induced by Tpp1$^{\Delta RD}$ (Rekha Rai, 2010; Robert T, 2011). We therefore asked whether Tpp1$^{\Delta RD}$-induced chromosome fusions differ in autophagy-competent and autophagy-deficient immortalized MEFs. Tpp1$^{\Delta RD}$ induced autophagic flux (**Figure 1E**) and chromosome fusions (**Figure 1F**). However, comparable numbers of fusions were observed in response to Tpp1$^{\Delta RD}$ expression independently of the autophagy status in *Atg5*$^{+/+}$ and

atg5$^{-/-}$ as well as in *Atg7*$^{+/+}$ and *atg7*$^{-/-}$ MEFs (**Figure 1G**, data not shown). Based on these cumulative results, we conclude that the autophagy pathway does not have an impact on the development of chromosome fusions induced by MT-mTER-47A and Tpp1$^{\Delta RD}$.

Figure 1

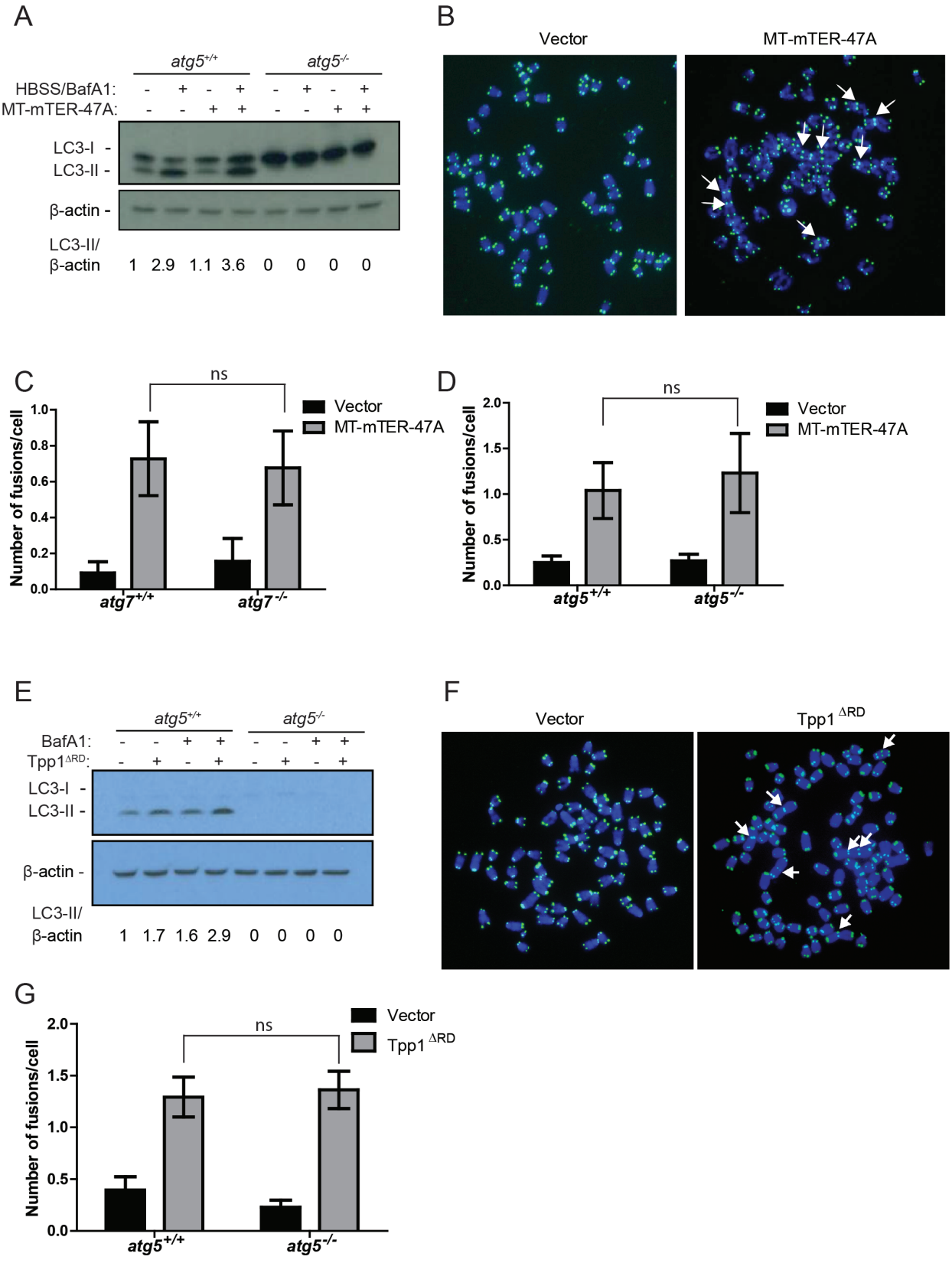
A
atg5+/+
atg5-/-
HBSS/BafA1:
MT-mTER-47A:
LC3-I -
LC3-II -
β-actin -
LC3-II/
β-actin
1 2.9 1.1 3.6 0 0 0 0
B
Vector
MT-mTER-47A
C
ns
Vector
MT-mTER-47A
Number of fusions/cell
atg7+/+
atg7-/-
D
ns
Vector
MT-mTER-47A
Number of fusions/cell
atg5+/+
atg5-/-
E
atg5+/+
atg5-/-
BafA1:
Tpp1ΔRD:
LC3-I -
LC3-II -
β-actin -
LC3-II/
β-actin
1 1.7 1.6 2.9 0 0 0 0
F
Vector
Tpp1 ΔRD
G
ns
Vector
Tpp1 ΔRD
Number of fusions/cell
atg5+/+
atg5-/-

Figure 1. Autophagy inhibition does not affect genomic instability following MT-mTER-47A or Tpp1$^{\Delta RD}$ transduction.

(**A**) LC3B immunoblot of MT-mTER-47A-treated immortalized MEFs expressing mouse TERT untreated or after 1.5 h of 25 nM $BafA_1$ and HBSS treatment. Relative amounts of LC3-II are indicated below the blots. (**B**) Representative images of chromosome fusions in Vector or MT-mTER-47A-treated cells. Arrows mark chromosome fusions. (**C,D**) Average number of chromosome fusions per cell in (**C**) *Atg5*$^{+/+}$ or matched *atg5*$^{-/-}$ immortalized MEFs, and (**D**) *Atg7*$^{+/+}$ or matched *atg7*$^{-/-}$ immortalized MEFs 6 days after MT-hTER-47A addition. (**E**) LC3B immunoblot of Tpp1$^{\Delta RD}$-treated immortalized MEFs untreated or after 1.5 h of 25 nM $BafA_1$. Relative amounts of LC3-II are indicated below the blots. (**F**) Representative images of chromosome fusions in Vector or Tpp1$^{\Delta RD}$-expressing cells. Arrows mark chromosome fusions. (G) Average number of chromosome fusions per cell in *Atg5*$^{+/+}$ or matched *atg5*$^{-/-}$ immortalized MEFs 6 days after transduction with Tpp1$^{\Delta RD}$. In all cases, MT-mTER-47A and Tpp1$^{\Delta RD}$ induced a significant amount of fusions compared to vector controls (P<0.01). In all cases a minimum of 1800 chromosomes were examined for chromosome fusions. Data is based on three or more parallel wells and is representative of at least 3 independent experiments. Error bars represent standard error. A 63X objective was used for metaphase imaging.

MATERIALS AND METHODS

Cell culture

Immortalized *Atg5*$^{+/+}$ and *atg5*$^{-/-}$ as well as *Atg7*$^{+/+}$ and *atg7*$^{-/-}$ MEFs were obtained from Noburu Mizushima (University of Tokyo) and Masaaki Komatsu (Tokyo Metropolitan Institute of Medical Science) respectively. Cells were cultured in Dulbecco modified Eagle medium medium (Invitrogen, 11965) supplemented with 10% FBS. All cells were grown at 37 ^{o}C in 5% CO2. For viral transduction, cells were infected for 24 h with lentivirus or 48 h with retrovirus, and antibiotic selection was started 24 h after virus removal at the following concentrations: puromycin (Life Technologies, A11138-02) at 1.5 ug/mL for 2 to 3 days.

Plasmids and viruses

Retroviral Tpp1$^{\Delta RD}$ plasmid was kindly provided by Sandy Chang (Yale University). The TER-expressing lentivector included a wild-type or mutant TER gene driven by the *IU1* promoter and a puromycin resistance gene driven by the *CMV* promoter (Shang Li, 2004). Lentiviral vectors expressing MT-mTER-47A and a retroviral vector-expressing mouse TERT were kindly provided by Amir Goldkorn (University of Southern California). Lentiviruses and retroviruses were produced as previously described (Bradley A. Stohr, 2010).

Fluorescent in situ hybridization (FISH)

To obtain metaphases, MEFs were treated with 0.1 µg/ml colcemid (Invitrogen, 15212) for 2 to 3 h. FISH was performed as previously described (Morgan E. Diolaiti, 2013). Telomeric DNA was detected with a PNA FISH probe (TMR-OO-5′-[CCCTAA]$_3$-3′, Panagene) and all images were obtained using a Metasystems Metafer slide scanning platform (70 Bridge Street Suite 100, Newton, MA 02458) in conjunction with a Zeiss Axio Imager Z2 upright microscope (5160 Hacienda Dr., Dublin, CA 94568) using a Zeiss 63X 1.4 NA Plan APOCHROMAT lens (5160 Hacienda Dr., Dublin, CA 94568) and Metafer software. Fusions were scored in a blinded fashion.

Autophagy assays

To examine autophagy flux, cells were treated with a single dose of BafA_1 (25 nM) (Sigma-Aldrich, B1793) for 1 h, E64d (10 ug/mL) and pepstatin A (10 ug/mL) for 5 h, or a vehicle control (DMSO or 100% ethanol) (Sigma-Aldrich, P5318, 11707, Enzo-PI107) as previously described (Elsa-Noah N'Diaye, 2009; Rebecca Locka, 2011). For starvation assays, cells were washed 3 times with phosphate-buffered saline (PBS) (Life Technologies, 14190) followed by HBSS (Invitrogen-14170) treatment for 1 h.

Immunoblotting

Cells were lysed in RIPA buffer supplemented with a protease and phosphatase-inhibitor cocktail (Thermo Scientific, 78440). Protein concentrations were determined using a BCA protein assay kit (Thermo Scientific 23225). Samples were run on 4-20% Tris-glycine gels after dilution in 2X Laemmli sample buffer supplemented with beta-

mercaptoethanol. Immunoblotting for LC3-II was performed with a 1:1000 dilution of LC3B antibody that has been previously described and is now commercially available (EMD Millipore, ABC232) (Christopher Fung, 2008). Immunoblotting for β-actin was performed using a 1:30,000 dilution of β-actin-HRP antibody (Abcam, ab20272). To quantify bands, Fiji software was used to measure band intensity of the protein of interest divided by the band intensity of β-actin.

Statistics

Data for chromosome fusions was analyzed using a nonparametric Kruskal-Wallis test, followed by a pairwise Wilcoxon signed-rank test with a Holm-Sidak correction for multiple comparisons. All statistical tests were done using R. Data was plotted using GraphPad Prism.

ACKNOWLEDGEMENTS

This research was funded in part by National Institutes of Health grant K08 CA134552 and by grant #IRG-97-150-14 from the American Cancer Society to BAS. This material is based upon work supported by the National Science Foundation under Grant No. 1144247 to FAM. We would like to thank Drs. Amir Goldkorn, Sandy Chang, and the Mizushima and the Komatsu laboratories for providing research materials.

CHAPTER 4

Implications and future directions

Content in this chapter was modified from the following publication:

Mar, FA, Debnath, J., Stohr BA. (2015). Autophagy-independent senescence and genome instability driven by targeted telomere dysfunction. *Autophagy, 11*(3): 527-37

DISCUSSION

Cellular senescence and chromosome fusions are two key outcomes of telomere dysfunction that critically affect tumor initiation and progression (Ding Z, 2012; Jerry W. Shay, 2005; Susan M. Bailey, 2006). Previous work in other systems has shown that telomere dysfunction induces autophagic flux (Hiroshi Aoki, 2007; Nicola Ivan Orlotti, 2012; Wen-Jun Zhou, 2009), and that autophagy regulates senescence and genome instability in some contexts (Andrew M. Leidal, 2012; Andrew R.J. Young, 2009; Robert T, 2011; Robin Mathew, 2007). Here, we have directly tested whether autophagy guides the response to acute telomere dysfunction. We find that while autophagic flux is indeed induced by several distinct types of telomere dysfunction, the resulting senescence and chromosome fusions are essentially unaffected by autophagy status.

The role of autophagy in the senescence response has been studied predominately in the context of oncogene activation. A previous study has uncovered that inhibition of autophagy delays the transition to senescence following overexpression of oncogenic $HRAS^{G12V}$ (Andrew R.J. Young, 2009), suggesting that autophagy induction promotes the senescent phenotype. A role for autophagy activation in promoting oncogene-induced senescence was subsequently identified in other systems (Andrew M. Leidal, 2012; Gewirtz, 2013). However, independent studies have found that the autophagy pathway can instead inhibit senescence in a variety of contexts (Hyun Tae Kang, 2011; Yihua Wanga, 2012). For example, autophagy inhibition in human fibroblasts triggers cellular senescence under certain conditions (Hyun Tae Kang, 2011), and knockdown of *ATG5* in mouse fibroblasts promotes Ras-

induced senescence (Yihua Wanga, 2012). These conflicting results could be due to a number of experimental differences, including the level of autophagy inhibition, the type of cells used, and the type of senescence trigger under study. Overall, the results from these studies reinforce that the connections between autophagy and cellular senescence remain complex and poorly defined (Gewirtz, 2013).

Our results described in Chapter 2 indicate that autophagy activation is not required for the transition to MT-hTER-47A-induced TDIS, thus providing additional evidence that senescence and autophagy are not always tightly linked. Moreover, previous studies of both $HRAS^{G12V}$ and v-cyclin-induced senescence have uncovered important roles for autophagy in the production of IL6 and IL8, two key SASP cytokines (Andrew M. Leidal, 2012; Andrew R.J. Young, 2009). In contrast to these models of OIS, we do not observe the robust elaboration of either cytokine in autophagy-competent or autophagy-deficient cells undergoing TDIS. This distinction between OIS and TDIS was a general feature of several types of TDIS and our results suggest that the SASP is more limited in the transition to TDIS than OIS. Interestingly, senescent cells that accumulate during wound healing also senesce in the absence of secreted IL6 (Marco Demaria, 2014).

It's important to note that our studies focus on the transition to senescence rather than the period of established senescence that occurs 10-14 days after introduction of the senescence trigger. Previous studies have compared the levels and composition of the SASP in fully senescent cells after oncogene expression and replicative exhaustion. In these studies, replicative senescent cells secrete SASP cytokines, but the secretory phenotype is one to six times weaker than the SASP observed in response to oncogene

expression. In addition, certain SASP factors were uniquely secreted by OIS cells (Jean-Philippe Coppé, 2008). These data, together with our findings examining the regulation of the SASP during the period of senescence transition, suggest that the senescence trigger may define the magnitude, composition, and time-dependent regulation of the SASP, which may in turn define the function of the senescent cell.

Building on the observation that, unlike OIS, transition to TDIS occurs in the absence of a robust SASP, we uncovered important differences in the levels and types of DNA damage in TDIS and OIS. First, OIS exhibits robust non-telomeric DNA damage while TDIS features more mild telomeric DNA damage. Previous studies have described the requirement for persistent DNA damage for the development of a SASP (Francis Rodier, 2009), but to our knowledge no study has closely examined the correlation between levels of DNA damage and the magnitude of the SASP during senescence transition. In preliminary data, we observed that the levels of phosphorylated-ATM but not phosphorylated-p53 correlate with levels of intracellular IL6 on a single cell basis. These data suggest that development of the SASP early in the transition to senescence is caused by robust signaling through the ATM pathway, but does not require p53 activation. In support of this idea, early studies of the SASP identified p53 as a factor that is dispensable for the development or maintenance of the SASP, but that restrains development of an amplified SASP (Jean-Philippe Coppé, 2008). In the absence of p53, the SASP was greater in magnitude and its development was accelerated (Jean-Philippe Coppé, 2008).

From these findings emerges the following speculative model. Oncogenes induce strong levels of ATM-dependent DNA damage signaling that in turn control the

establishment of the SASP. On the other hand, ATM-dependent DNA damage signaling induced by telomere dysfunction is sufficient to induce senescence but is milder in nature, specifically localized to telomeres, and is not sufficient to induce the robust SASP observed upon expression of oncogenes. The different levels of the SASP during the period of senescence transition in OIS and TDIS may partly explain the different requirements for the autophagy pathway in mediating these two types of senescence. In addition, different levels of secreted SASP factors in response to OIS and TDIS may define the function of the senescent cell.

Cells experiencing telomere dysfunction accumulate chromosome fusions, resulting in significant genome instability (Murnane, 2012; Wilhelm Palm, 2008). Initial studies examining the role of autophagy in genome stability conclude that autophagy suppresses chromosome instability by maintaining cellular metabolic homeostasis (Robin Mathew, 2007). Subsequent work has suggested that autophagy also modulates genome stability by controlling DNA damage repair mechanisms and cell cycle progression. In yeast, autophagy targets the DNA damage repair protein Sae2 (orthologous to human CtIP) for autophagic degradation upon its acetylation (Robert T, 2011), and autophagy has also been implicated in regulating levels of CtIP in human colon cancer cells (Praveen Rajendran, 2013). These data suggest that autophagy may control DNA damage repair in mammalian cells through the regulation of CtIP, a key protein mediating the choice between nonhomologous and homologous repair pathways (Maximina Yun, 2009). Autophagy has also been shown to influence cell cycle progression. For example, studies in yeast have shown that modulating autophagy upon

nutrient starvation causes a delay in cell cycle progression and defects in nuclear division, leading to aneuploidy (Aiko Matsui, 2013). In mammals, autophagy regulates protein levels of active RHOA in a SQSTM1/p62-dependent manner. When autophagy is disrupted, active RHOA accumulates in areas surrounding the midbody and causes cytokinesis failure, multinucleation, and aneuploidy (Amine Belaid, 2013). While changes in DNA repair mechanisms and cell cycle progression could potentially influence the extent and pattern of telomere fusions, our results described in Chapter 3 show no change in these readouts despite the complete loss of autophagic activity in immortalized *atg5* or *atg7* knockout MEFs. Thus, autophagy does not influence telomere dysfunction-induced genome instability in this cellular context.

FUTURE DIRECTIONS

This study raises a number of new interesting questions we believe are worth pursuing. Important questions for future study include determining whether autophagy serves critical functions in other types of senescence, such as that induced by CDKN2A overexpression (Jean-Philippe Coppé, 2011), and whether the impact of autophagy on different kinds of senescence parallels the level of key SASP mediators involved in each. In addition, it will be important to establish whether the role of autophagy in senescence differs between the mesenchymal cells used in this study and various epithelial cell types that also undergo telomere dysfunction-induced cell cycle arrest, such as HMECs (Paul Yaswen, 2002). In order to further examine the signaling

pathways controlling the development of the SASP and how they may differ based on the senescence trigger, experiments will have to be conducted to verify the finding that IL6 correlates with levels of phosphorylated-ATM but not phosphorylated-p53.

While our study defines the autophagy-independent nature of chromosome fusions triggered by telomere dysfunction, our results do not rule out a role for autophagy in repair of other DNA lesions at telomeres or throughout the rest of the genome, including those that rely on homologous recombination for resolution. Because autophagy controls the levels of several proteins involved—directly or indirectly—in DNA damage repair, future studies should investigate the role of autophagy in the repair of other types of DNA lesions.

CLINICAL IMPLICATIONS

As autophagy inhibitors reach the clinic for the treatment of a variety of cancers, it is critical to understand how these therapeutic agents affect basic cellular processes that influence cancer initiation and progression, including the dysfunctional telomere response. While autophagy inhibition for the purposes of anticancer therapy may impinge on a variety of cellular pathways, potentially eliciting unwanted side effects, our results suggest that impaired autophagy is unlikely to alter the acute response to telomere dysfunction.

REFERENCES

Aiko Matsui, Y.K., Akira Matsuura (2013). The Role of Autophagy in Genome Stability through Suppression of Abnormal Mitosis under Starvation PLOS Genetics *9*.

Amine Belaid, M.C., Abderrahman Chargui, Elisabeth Corcelle, Termeau, Florence Pedeutour, Sandy Giuliano, Marius Ilie, Isabelle Rubera, Michel Tauc, Sophie Barale, Corinne Bertolotto, Patrick Brest, Valerie Vouret-Craviari, Daniel J. Klionsky, Georges F. Carle, Paul Hofman, Baharia Mograbi (2013). Autophagy plays a critical role in the degradation of active RHOA, the control of cell cytokinesis, and genomic stability. Cancer Research *73*, 11.

Andrea G. Bodnar, M.O., Maria Frolkis, Shawn E. Holt, Choy-Pik Chiu, Gregg B. Morin, Calvin B. Harley, Jerry W. Shay, Serge Lichtsteiner, Woodring E. Wright (1998). Extension of life-span by introduction of telomerase into normal human cells. Science *279*, 3.

Andrew M. Leidal, D.P.C., Richard J. Hill, Patrick W.K. Lee, Craig McCormick (2012). Subversion of Autophagy by Kaposi's Sarcoma-Associated Herpesvirus Impairs Oncogene-Induced Senescence. Cell Host & Microbe *11*, 13.

Andrew R.J. Young, M.N., Manuela Ferreira, Kristina Kirschner, Mahito Sadaie, Jeremy F.J. Darot, Simon Tavaré, Satoko Arakawa, Shigeomi Shimizu, Fiona M. Watt, Masashi Narita (2009). Autophagy mediates the mitotic senescence transition. Genes and Development *23*, 5.

Anitha Suram, J.K., Priyanka L Patel, Haihe Ruan, Aurora Cerutti, Virginia Boccardi, Marzia Fumagalli, Raffaella Di Micco, Neena Mirani, Resham Lal Gurung, Manoor Prakash Hande, Fabrizio d'Adda di Fagagna, Utz Herbig (2012). Oncogene-induced telomere dysfunction enforces cellular senescence in human cancer precursor lesions. EMBO *31*, 22.

Bradley A. Stohr, E.H.B. (2008). ATM mediates cytotoxicity of a mutant telomerase RNA in human cancer cells. Cancer Research *68*, 8.

Bradley A. Stohr, L.X., Elizabeth H. Blackburn (2010). The terminal telomeric DNA sequence determines the mechanism of dysfunctional telomere fusion. Molecular Cell *39*, 7.

Carmen Martin-Ruiz, G.S., Joanne Petrie, Juliane Ladhoff, Jessie Jeyapalan, Wenyi Wei, John Sedivy, Thomas von Zglinicki (2004). Stochastic variation in telomere shortening rate causes heterogeneity of human fibroblast replicative life span. Journal of Biological Chemistry *279*, 7.

Christian M. Beauséjour, A.K., Francesco Galimi, Masashi Narita, Scott W. Lowe, Paul Yaswen, Judith Campisi (2003). Reversal of human cellular senescence: roles of the p53 and p16 pathways. EMBO Journal *22*, 10.

Christopher Fung, R.L., Sizhen Gao, Eduardo Salas, Jayanta Debnath (2008). Induction of autophagy during extracellular matrix detachment promotes cell survival. Molecular Biology of the Cell *19*, 9.

Chrysiis Michaloglou, L.C.W.V., Maria S. Soengas, Christophe Denoyelle, Thomas Kuilman, Chantal M. A. M. van der Horst, Donné M. Majoor, Jerry W. Shay, Wolter J. Mooi, Daniel S. Peeper (2005). BRAFE600-associated senescence-like cell cycle arrest of human naevi. Nature *436*, 4.

Debnath, L.M.J. (2013). Autophagy as a stress-response and quality-control mechanism: implications for cell injury and human disease. Annual Reviews Pathology *8*, 32.

Ding Z, W.C., Jaskelioff M, Ivanova E, Kost-Alimova M, Protopopov A, Chu GC, Wang G, Lu X, Labrot ES, Hu J, Wang W, Xiao Y, Zhang H, Zhang J, Zhang J, Gan B, Perry SR, Jiang S, Li L, Horner JW, Wang YA, Chin L, DePinho RA. (2012). Telomerase reactivation following telomere dysfunction yields murine prostate tumors with bone metastases. Cell *148*, 11.

Elsa-Noah N'Diaye, K.K.K., Ivy Hsieh, Hiroshi Morisaki, Jayanta Debnath, Eric J Brown (2009). PLIC proteins or ubiquilins regulate autophagy-dependent cell survival during nutrient starvation. EMBO Reports *10*, 6.

Eros Lazzerini Denchi, T.d.L. (2007). Protection of telomeres through independent control of ATM and ATR by TRF2 and POT1. Nature *338*, 3.

Fabrizio d'Adda di Fagagna, P.M.R., Lorena Clay-Farrace, Heike Fiegler, Philippa Carr, Thomas von Zglinicki, Gabriele Saretzki, Nigel P. Carter, Stephen P. Jackson (2003). A DNA damage checkpoint response in telomere-initiated senescence. Nature *426*, 4.

Florence Debacq-Chainiaux, J.D.E., Judith Campisi, Olivier Toussaint (2009). Protocols to detect senescence-associated beta-galactosidase (SA-betagal) activity, a biomarker of senescent cells in culture and in vivo. Nature Protocols *4*, 8.

Francis Rodier, J.-P.C., Christopher K. Patil, Wieteke A. M. Hoeijmakers, Denise P. Muñoz, Saba R. Raza, Adam Freund, Eric Campeau, Albert R. Davalos, Judith Campisi (2009). Persistent DNA damage signalling triggers senescence-associated inflammatory cytokine secretion. Nature Cell Biology *11*, 4.

Franklin W. Huang, E.H., Mary Jue Xu, Gregory V. Kryukov, Lynda Chin, Levi A. Garraway (2013). Highly recurrent TERT promoter mutations in human melanoma. Science *339*, 3.
Gewirtz, D.A. (2013). Autophagy and senescence: a partnership in search of definition. Autophagy *9*, 4.

Guido Kroemer, G.M., Beth Levine (2010). Autophagy and the integrated stress response. Molecular Cell *40*, 13.

Haferkamp S, T.S., Becker TM, Scurr LL, Kefford RF, Rizos H. (2009). The relative contributions of the p53 and pRb pathways in oncogene-induced melanocyte senescence. Aging *1*, 14.

Hiroshi Aoki, E.I., Mark S. Eller, Yasuko Kondo, Keishi Fujiwara, Guang-Zhi Li, Kenneth R. Hess, Doris R. Siwak, Raymond Sawaya, Gordon B. Mills, Barbara A. Gilchrest, Seiji Kondo (2007). Telomere 3′ overhang-specific DNA oligonucleotides induce autophagy in malignant glioma cells. FASEB Journal *21*, 22.

Hyun Tae Kang, K.B.L., Sung Young Kim, Hae Ri Choi, Sang Chul Park (2011). Autophagy impairment induces premature senescence in primary human fibroblasts. PLOS One *6*.
Ian R. Kill, R.G.A.F., Kay Lawrence, Sydney Shall (1994). The expression of proliferation-dependent antigens during the lifespan of normal and progeroid human fibroblasts in culture. Journal of Cell Science *2*, 8.

Jan Karlseder, A.S., Titia de Lange (2002). Senescence induced by altered telomere state, not telomere loss. Science *295*, 3.

Jean-Philippe Coppé, C.K.P.e.c., Francis Rodier equal contributor, Yu Sun, Denise P Muñoz, Joshua Goldstein, Peter S Nelson, Pierre-Yves Desprez, Judith Campisi (2008). Senescence-Associated Secretory Phenotypes Reveal Cell-Nonautonomous Functions of Oncogenic RAS and the p53 Tumor Suppressor PLOS Biology *6*, 15.

Jean-Philippe Coppé, F.R., Christopher K. Patil, Adam Freund, Pierre-Yves Desprez, Judith Campisi (2011). Tumor suppressor and aging biomarker p16(INK4a) induces cellular senescence without the associated inflammatory secretory phenotype. Journal of Biological Chemistry *286*, 7.

Jerry W. Shay, W.E.W. (2005). Senescence and immortalization: role of telomeres and telomerase. Carcinogenesis *26*, 7.

Jirina Bartkova, N.R., Michalis Liontos, Panagiotis Karakaidos, Dimitris Kletsas, Natalia Issaeva, Leandros-Vassilios F. Vassiliou, Evangelos Kolettas, Katerina Niforou, Vassilis C. Zoumpourlis, Munenori Takaoka, Hiroshi Nakagawa, Frederic Tort, Kasper Fugger, Fredrik Johansson, Maxwell Sehested, Claus L. Andersen, Lars Dyrskjot, Torben Ørntoft, Jiri Lukas, Christos Kittas, Thomas Helleday, Thanos D. Halazonetis, Jiri Bartek, Vassilis G. Gorgoulis (2006). Oncogene-induced senescence is part of the tumorigenesis barrier imposed by DNA damage checkpoints. Nature *444*, 4.

João Vinagre, A.A., Helena Pópulo, Rui Batista, Joana Lyra, Vasco Pinto, Ricardo Coelho, Ricardo Celestino, Hugo Prazeres, Luis Lima, Miguel Melo, Adriana Gaspar da Rocha, Ana Preto, Patrícia Castro,Ligia Castro, Fernando Pardal, José Manuel Lopes, Lúcio Lara Santos, Rui Manuel Reis, José Cameselle-Teijeiro, Manuel Sobrinho-Simões, Jorge Lima, Valdemar Máximo, Paula Soares (2013). Frequency of TERT promoter mutations in human cancers. Nature Communications *4*.

Juan Carlos Acosta, A.B., Torsten Wuestefeld, Athena Georgilis, Peggy Janich, Jennifer P. Morton, Dimitris Athineos, Tae-Won Kang, Felix Lasitschka, Mindaugas Andrulis, Gloria Pascual, Kelly J. Morris, Sadaf Khan, Hong Jin, Gopuraja Dharmalingam, Ambrosius P. Snijders, Thomas Carroll, David Capper, Catrin Pritchard, Gareth J. Inman, Thomas Longerich, Owen J. Sansom, Salvador Aznar Benitah, Lars Zender, Jesús Gil (2013). A complex secretory program orchestrated by the inflammasome controls paracrine senescence. Nature Cell Biology *15*, 12.

L. Hayflick, P.S.M. (1961). The serial cultivation of human diploid cell strains. Experimental Cell Research *25*, 36.

Lange, T.D. (2005). Teloemre-related genome instability in cancer. Cold Spring Harbor Symposia on Quantitative Biology *70*, 8.

Lidija Marusic, M.A., Antonella Tidy, Ping Wang, Bryant Villeponteau, Silvia Bacchetti (1997). Reprogramming of telomerase by expression of mutant telomerase RNA template in human cells leads to altered telomeres that correlate with reduced cell viability. Molecular Cell Biology *17*, 7.

Ludovic Deriano, D.B.R. (2013). Modernizing the nonhomologous end-joining repertoire: alternative and classical NHEJ share the stage. Annual Reviews Genetics *47*, 22.

Manuel Serrano, A.W.L., Mila E McCurrach, David Beachemail, Scott W Lowe (1997). Oncogenic ras Provokes Premature Cell Senescence Associated with Accumulation of p53 and p16INK4a. Cell *88*, 9.

Marco Demaria, N.O., Sameh A. Youssef, Francis Rodier, Wendy Toussaint, James R. Mitchell, Remi-Martin Laberge, Jan Vijg, Harry Van Steeg, Martijn E.T. Dollé, Jan H.J. Hoeijmakers, Alain de Bruin, Eiji Hara, Judith Campisi (2014). An essential role for senescent cells in optimal wound healing through secretion of PDGF-AA. Developmental Cell *31*, 13.

Masako Narita, A.R.J.Y., Satoko Arakawa, Shamith A. Samarajiwa, Takayuki Nakashima, Sei Yoshida, Sungki Hong, Lorraine S. Berry, Stefanie Reichelt, Manuela Ferreira, Simon Tavaré, Ken Inoki, Shigeomi Shimizu, Masashi Narita (2011). Spatial Coupling of mTOR and Autophagy Augments Secretory Phenotypes. Science *332*, 4.

Maximina Yun, K.H. (2009). CtIP-BRCA1 modulates the choice of DNA double-strand-break repair pathway throughout the cell cycle. Nature *459*, 3.

Melanie Braig, S.L., Christoph Loddenkemper, Cornelia Rudolph, Antoine H.F.M. Peters, Brigitte Schlegelberger, Harald Stein, Bernd Dörken, Thomas Jenuwein, Clemens A. Schmitt (2005). Oncogene-induced senescence as an initial barrier in lymphoma development. Nature *436*, 5.

Morgan E. Diolaiti, B.A.C., Robin Kageyama, Florie A. Charles, Bradley A. Stohr (2013). In situ visualization of telomere elongation patterns in human cells Nuclei Acids Research *41*, 9.

Moses M. Kim, M.A.R., Inna L. Botchkina, Refaat Shalaby, Ann D. Thor, Elizabeth H. Blackburn (2001). A low threshold level of expression of mutant-template telomerase RNA inhibits human tumor cell proliferation. PNAS *98*, 5.

Murnane, J.P. (2012). Telomere dysfunction and chromosome instability. Mutation Research *730*, 8.

Nelson DM, M.T., Jeyapalan JC, Sedivy JM, Adams PD. (2014). A comparison of oncogene-induced senescence and replicative senescence: implications for tumor suppression and aging. Age.

Nicola Ivan Orlotti, G.C.-R., Erika Borghini, Marzia Pennati, Claudia Sissi, Federica Perrone, Manlio Palumbo, Maria Grazia Daidone, Marco Folini, Nadia Zaffaroni (2012). Autophagy acts as a safeguard mechanism against G-quadruplex ligand-mediated DNA damage. Autophagy *8*, 9.

Noboru Mizushima, T.Y., Beth Levine (2010). Methods in mammalian autophagy research. Cell *140*, 13.

Patrick J. Killelaa, Z.J.R., Yuchen Jiaob, Chetan Bettegowda, Nishant Agrawal, Luis A. Diaz, Jr., Allan H. Friedman, Henry Friedman, Gary L. Gallia, Beppino C. Giovanella, Arthur P. Grollman, Tong-Chuan He, Yiping He, Ralph H. Hruban, George I. Jallo, Nils Mandahl, Alan K. Meeker, Fredrik Mertens, George J. Netto, B. Ahmed Rasheed, Gregory J. Riggins, Thomas A. Rosenquist, Mark Schiffman, Ie-Ming Shih, Dan Theodorescu, Michael S. Torbenson, Victor E. Velculescu, Tian-Li Wang, Nicolas Wentzensen, Laura D. Wood, Ming Zhang, Roger E. McLendon, Darell D. Bigner, Kenneth W. Kinzler, Bert Vogelstein, Nickolas Papadopoulos, Hai Yan (2013). TERT promoter mutations occur frequently in gliomas and a subset of tumors derived from cells with low rates of self-renewal. PNAS *9*, 6.

Paul Yaswen, M.R.S. (2002). Molecular changes accompanying senescence and immortalization of cultured human mammary epithelial cells. The International Journal of Biochemistry & Cell Biology *34*, 8.

Peter Krutzik, G.N. (2003). Intracellular Phospho-protein Staining Techniques for Flow Cytometry: Monitoring Single Cell Signaling Events. Cytometry A *55*, 10.

Praveen Rajendran, A.I.K., Tian-Wei Yu, Wan-Mohaiza Dashwood, William H. Bisson, Christiane V. Löhr, Emily Ho, David E. Williams, Roderick H. Dashwood (2013). HDAC turnover, CtIP acetylation and dysregulated DNA damage signaling in colon cancer cells treated with sulforaphane and related dietary isothiocyanates. Epigenetics *8*, 11.

Raffaella Di Micco, M.F., Angelo Cicalese, Sara Piccinin, Patrizia Gasparini, Chiara Luise, Catherine Schurra, Massimiliano Garre', Paolo Giovanni Nuciforo, Aaron Bensimon, Roberta Maestro, Pier Giuseppe Pelicci, Fabrizio d'Adda di Fagagna (2006). Oncogene-induced senescence is a DNA damage response triggered by DNA hyper-replication. Nature *444*, 4.

Rebecca Locka, S.R., Candia M. Kenifica, Judy S. Suc, Eduardo Salasa, Sabrina M. Ronen, Jayanta Debnath (2011). Autophagy facilitates glycolysis during Ras-mediated oncogenic transformation. Molecular Biology of the Cell *22*, 13.

Rekha Rai, H.Z., Hua He, Ying Luo, Asha Multani, Phillip B Carpenter, Sandy Chang (2010). The function of classical and alternative non-homologous end-joining pathways in the fusion of dysfunctional telomeres. EMBO Journal *29*, 12.

Robert J. A. Bell, H.T.R., Alex Kreig, Andrew Mancini, Shaun F. Fouse, Raman P. Nagarajan, Serah Choi, Chibo Hong, Daniel He, Melike Pekmezci, John K. Wiencke, Margaret R. Wrensch, Susan M. Chang, Kyle M. Walsh, Sua Myong, Jun S. Song, Joseph F. Costello (2015). The transcription factor GABP selectively binds and activates the mutant TERT promoter in cancer. Science.

Robert T, V.F., Chiolo I, Shubassi G, Bernstein KA, Rothstein R, Botrugno OA, Parazzoli D, Oldani A, Minucci S, Foiani M. (2011). HDACs link the DNA damage response, processing of double-strand breaks and autophagy. Nature *471*, 74-79.

Robin Mathew, S.K., Brian Beaudoin, Cristina M. Karp, Kevin Bray, Kurt Degenhardt, Guanghua Chen, Shengkan Jin, and Eileen White (2007). Autophagy suppresses tumor progression by limiting chromosomal instability. Genes and Development *21*, 14.

Shang Li, J.E.R., Annemarie A. Donjacour, Inna L. Botchkina, Yun Kit Hom 2, Gerald R. Cunha, Elizabeth H. Blackburn (2004). Rapid inhibition of cancer cell growth induced by lentiviral delivery and expression of mutant-template telomerase RNA and anti-telomerase short-interfering RNA. Cancer Research *64*, 7.

Sumit Borah, L.X., Arthur J. Zaug, Natasha M. Powell, Garrett M. Dancik, Scott B. Cohen, James C. Costello, Dan Theodorescu, Thomas R. Cech (2015). TERT promoter mutations and telomerase reactivation in urothelial cancer Science *347*, 5.

Susan M. Bailey, J.P.M. (2006). Telomeres, chromosome instability and cancer. Nucleic Acids Research *34*, 9.

Susanne Horn, A.F., P. Sivaramakrishna Rachakonda, Christine Fischer, Antje Sucker, Andreas Gast, Stephanie Kadel, Iris Moll, Eduardo Nagore, Kari Hemminki, Dirk Schadendorf, Rajiv Kumar (2013). TERT promoter mutations in familial and sporadic melanoma. Science *339*, 3.

Thomas Kuilman, C.M., Liesbeth C.W. Vredeveld, Sirith Douma, Remco van Doorn, Christophe J. Desmet, Lucien A. Aarden, Wolter J. Mooi, Daniel S. Peeperemail (2008).

Oncogene-Induced Senescence Relayed by an Interleukin-Dependent Inflammatory Network. Cell *133*, 12.

Wen-Jun Zhou, R.D., Xiao-Yue Zhang, Gong-Kan Feng, Lian-Quan Gu, Xiao-Feng Zhu (2009). G-quadruplex ligand SYUIQ-5 induces autophagy by telomere damage and TRF2 delocalization in cancer cells. Molecular Cancer Therapeutics *8*, 10.

Wilhelm Palm, T.d.L. (2008). How shelterin protects mammalian telomeres. Annual Review of Genetics *42*, 333.

Yihua Wanga, X.D.W., Eleonora Lapia, Alexandra Sullivana, Wei Jiab, You-Wen Heb, Indrika Ratnayakaa, Shan Zhonga, Robert D. Goldinc, Christoph G. Goemansd, Aviva M. Tolkovskyd, Xin Lua (2012). Autophagic activity dictates the cellular response to oncogenic RAS. PNAS *109*, 5.

Zhenbang Chen, L.C.T., David Shaffer, Hui-Kuan Lin, Zohar A. Dotan, Masaru Niki, Jason A. Koutcher, Howard I. Scher, Thomas Ludwig, William Gerald, Carlos Cordon-Cardo, Pier Paolo Pandolfi (2005). Crucial role of p53-dependent cellular senescence in suppression of Pten-deficient tumorigenesis. Nature *436*, 5.

Publishing Agreement

It is the policy of the University to encourage the distribution of all theses, dissertations, and manuscripts. Copies of all UCSF theses, dissertations, and manuscripts will be routed to the library via the Graduate Division. The library will make all theses, dissertations, and manuscripts accessible to the public and will preserve these to the best of their abilities, in perpetuity.

Please sign the following statement:

I hereby grant permission to the Graduate Division of the University of California, San Francisco to release copies of my thesis, dissertation, or manuscript to the Campus Library to provide access and preservation, in whole or in part, in perpetuity.

Author Signature

6/19/15

Date